UNIVERSITAT POLITÈCNICA DE CATALUNYA

Department of Chemical Engineering

ENERGY OPTIMISATION AND CONTROLLABILITY IN COMPLEX DISTILLATION COLUMNS

Autor: Maria Serra i Prat
Director: Miquel Perrier

Barcelona, june 2000

CHAPTER 4. MIMO FEEDBACK CONTROL ANALYSIS OF THE DIVIDED WALL COLUMN

4.1 Abstract

This chapter addresses the stabilisation and the composition control of the DWC through decentralised feedback control. The scope of preliminary works addressing decentralised feedback control in the DWC is further extended to analyse the DWC control design in detail. In order to find out which are the best control structures, different control structures are systematically analysed and compared under performance and robustness criteria. Linear analysis tools are used for the Multiple Input Multiple Output (MIMO) feedback control analysis and non-linear models are used for simulations. The tuning of Proportional Integral (PI) controllers is discussed. Performance improvement through the transformation of the composition controlled variables into logarithms is considered. The effect of the energy optimisation on the controllability of the DWC is evaluated comparing optimal nominal operating conditions with non-optimal nominal operating conditions. In order to test the generality of the results, different case studies including different designs and separation problems are analysed.

4.2 Introduction

As was seen in chapter two, thermal coupling and correct thermodynamic distillation sequence are the main reasons why the DWC energy consumption is lower than the energy consumption of the conventional arrangements for ternary separations. These conditions can be met thanks to the complex design of the DWC, which offers extra operation DOF. Because of the DWC complexity, it has more candidate control variables than the conventional distillation arrangements. Therefore, the possible control structures are different and the control of the DWC arrangement is a new subject of study. In addition, the DWC applications in the literature (see chapter three) indicate moderate to high purity products, with their associated complications due to non-linearity and large time constants.

The general control objectives considered in this thesis work are the column stabilisation, to maintain the purity of the three products at the setpoints, and to maintain the operation close to

minimum energy consumption. In chapters four and five, the stabilisation and the composition control of the DWC are studied. Chapter six will address the DWC optimising control.

As seen in chapters two and three, since its design was proposed almost fifty years ago, many authors have addressed DWC design considerations. Operation and control of the DWC have received much less attention. However, some works have been published recently. Preliminary results reported indicate that decentralised feedback control structures may be used to control the DWC and acceptable control seems feasible. Since decentralised feedback control is the simplest control strategy, it has been the first control strategy under concern in this thesis work.

Wolff et al. (1995) considered the operation and control of the Petlyuk Column. Linear analysis tools and frequency-dependent plots were used to study the *L S V* control structure in a decentralised feedback control strategy. This control structure consists in the control of A purity (x_{AD}) by *L*, the control of B purity (x_{BS}) by *S*, and the control of C purity (x_{CB}) by *V* (see Figure 2.16). From a linear point of view, they did not find major problems with the *L S V* control structure. However, they found serious problems related to the steady state behaviour if four compositions were specified and concluded that "holes" in the operation range would make it very difficult to control four compositions.

Annakou et al. (1996 b) compared the controllability of the heat integrated column sequences and the fully thermally coupled distillation column (Petlyuk Column). Through degrees of freedom analysis and steady state multivariable control synthesis tools, they showed that both investigated schemes could be controlled by conventional decentralised control structures, although interaction among control loops was smaller for the heat integrated system.

Abdul et al. (1998) also studied the operation and control of the DWC. They suggested that both liquid and vapour splits (*SPLITD* and *SPLITB*) were maintained constant at their nominal values. Two control structures were considered in their work: *L S V* and *D S V*. The second one consists in the control of A purity by *D*, the control of B purity by *S*, and the control of the C purity by *V*. The steady state Relative Gain Array (***RGA***) of the two control schemes was calculated to make an interaction analysis and simulations showed, according to the ***RGA*** results, that *D S V* control structure is better than *L S V* control structure.

Doukas et al. (1981) studied two control schemes for the "Petlyuk Column" without thermal coupling. Since this arrangement does not have split variables, the control problem is different. However, the way the authors proposed to control x_{BS} through the localisation of the product tray is interesting and could be applied to the DWC.

Results obtained in the literature up to now valorise positively decentralised feedback control application to the DWC. However, further analysis will be very interesting. Basically, the objective of this chapter is to search the best control structures and the best operating conditions offered by the DWC complexity. Importance is given to the inventory control structure and to

the fact that, having the DWC large reflux ratios, the inventory control structure consisting in the manipulation of D and B may have serious problems to achieve stabilisation.

4.3 The models

In this chapter, non-linear and linear models of the DWC are developed and used to study and simulate the DWC. For the easy manipulation of the transfer functions, reduced linear models have also been used.

4.3.1 The non-linear model

The non-linear model is used to simulate the behaviour of the controlled DWC. On the other hand, it is the base for the calculation of the linear model.

4.3.1.1 Non-linear model assumptions

During the modelling task, the level of detail of the model is determined. It is important to find an adequate model for each purpose. In chemical engineering process control, high frequencies are out of interest because the control system does not respond to high frequency signals. Since the frequency response in the range of interest is essentially independent of extraneous model detail (with high frequency effects), models contemplating a lot of detail are nonsense.

In accordance with the distillation model for the control study of a binary simple distillation column proposed by Skogestad (1997), the following set of assumptions have been considered. These assumptions will give a quite simple model, which will contain the essential elements driving the control system:

- constant pressure
- constant relative volatility of components
- constant molar flows through the column sections
- no vapour holdup
- linear liquid dynamics
- equilibrium in all stages

Of all the assumptions, constant pressure has the largest effect on the control system. When considering the pressure, also its control has to be considered. In most distillation columns, the vapour entering the condenser is used for pressure control.

4.3.1.2 Non-linear model description

The developed model is based on the mass balance and equilibrium equations, which apply to every tray. Energy balance equations are not used. Instead, constant vapour molar flows are assumed through the column sections at steady state.

The equations for the mass balance at any regular tray i are indicated in equations 4.1 and 4.2, where v is vapour flowrate, l is liquid flowrate, $l0$ is the nominal liquid flowrate, M is the holdup, $M0$ is the nominal holdup and τ is the time constant for the liquid flow dynamics in minutes. v(i), l(i) and $l0$(i) are the flowrates leaving tray i.

$$v(i) = v(i\text{-}1) \qquad (4.1)$$

$$l(i) = l0(i) + (M(i) - M0(i))/\tau \qquad (4.2)$$

As indicated by equation 4.1, the model does not simulate vapour dynamics. However, as indicated by equation 4.2, the model simulates liquid dynamics. The liquid leaving a tray increases with the liquid holdup. The ratio is given by τ.

In 4.3 and 4.4, the vapour-liquid equilibrium equations at tray i are shown, where y_A is the equilibrium A vapour fraction, x_A is the equilibrium A liquid fraction, and the same for y_B, x_B, y_C, and x_C.

$$y_A(i) = \frac{\alpha_2 * x_A(i)}{\alpha_1 * x_A(i) + \alpha_2 * x_B(i) + \alpha_3 * x_C(i)} \qquad (4.3)$$

$$y_B(i) = \frac{\alpha_2 * x_B(i)}{\alpha_1 * x_A(i) + \alpha_2 * x_B(i) + \alpha_3 * x_C(i)} \qquad (4.4)$$

Regarding the dynamics, three differential equations are solved at every column tray. They are the total mass balance, and component A and B mass balances. In 4.5, 4.6, and 4.7, these equations for the regular trays are shown, where Mx_A and Mx_B are $M*x_A$ and $M*x_B$.

$$\frac{dM}{dt}(i) = l(i+1) - l(i) + v(i-1) - v(i) \qquad (4.5)$$

$$\frac{dMx_A}{dt}(i) = l(i+1) * x_A(i+1) - l(i) * x_A(i) + v(i-1) * y_A(i-1) - v(i) * y_A(i) \qquad (4.6)$$

$$\frac{dMx_B}{dt}(i) = l(i+1) * x_B(i+1) - l(i) * x_B(i) + v(i-1) * y_B(i-1) - v(i) * y_B(i) \qquad (4.7)$$

The derivatives of the composition variables are calculated from the derivatives of the mass variables according to equations 4.8 and 4.9.

$$\frac{dx_A}{dt}(i) = \frac{\frac{dMx_A}{dt}(i) - x_A(i) * \frac{dM}{dt}(i)}{M(i)} \qquad (4.8)$$

$$\frac{dx_B}{dt}(i) = \frac{\frac{dMx_B}{dt}(i) - x_B(i) * \frac{dM}{dt}(i)}{M(i)} \qquad (4.9)$$

Based on equations 4.1 to 4.9, a DMC model is built, which has been programmed in MATLAB (MATLAB, 1998). The model calculates the derivatives of the state variables ($x_A(i)$, $x_B(i)$, and $M(i)$) when the values of the state variables are given to it. Ode15s MATLAB file, which has a variant step time and is appropriate for stiff systems, is used to integrate the differential equations and obtain this way the dynamic simulation of the process. Advantage is taken of SIMULINK to simulate and obtain results.

The inputs of the model are the reflux flowrate L, the boilup V, the distillate flowrate D, the bottoms flowrate B, the sidestream flowrate S, the split of liquid *SPLITD*, the split of vapour *SPLITB*, the feed flowrate F, the A molar fraction in feed stream z_A, the B molar fraction in feed stream z_B, and the feed liquid fraction q_F. A scheme of the modelled DWC can be seen in Figure 2.16.

In the model, the stabilisation of the process (mass balance=0) is not imposed. Two control loops will be responsible of the column stabilisation or inventory control. Specifically, the stabilisation loops will control the liquid levels in the condenser and reflux drum ($M(1)$ and $M(NM)$). The size of these two tanks influences the liquid dynamics.

Considering the tank levels as state variables, the effect of the tuning of their control can be studied. In the contrary case, perfect control should have been assumed. Consideration of the tray holdups as state variables, or in other words, consideration of the liquid dynamics, introduces a delay in the output responses which has an important effect in the control. It imposes that some time it taken from when a change in the liquid flowrate occurs in the top of the column until this change arrives the reboiler (see equation 4.2). τ is the hydraulic lag on each theoretical tray. And specifically, $(NM\text{-}1)*\tau$ is the time it takes for an increase in reflux to affect the reboiler level. For instance, for a column with NM=40 and τ=0.063, it will take 40*(0.063 min)=2.52 min. This overall lag for liquid response is a good control property because with sufficiently fast control, some strong interactions that exist at steady state between the compositions at the top and the bottom of the column can be avoided. In other words, the initial high-frequency response is decoupled.

It is important to notice that, although the liquid dynamics imposes a lag to the column response, mathematically, a delay is not represented by the model equations. For the model, initial increments travel instantaneously through the column.

A separation example

A separation example is chosen to illustrate the explications about the model, which will also be used in other sections of this and coming chapters.

The chosen DWC design has NT=40, NP=10, NM=30, NS=15, NCB=7, NCD=23 and NF=5. This is a symmetric design, which has not been optimised.

The ternary mixture to be separated has α=(4.65:2.15:1). The nominal feed conditions are:

- z_A=0.333 molar, z_B=0.333 molar (equimolar mixture)
- feed flowrate F=1 kmol/min
- liquid feed q_F=1 (saturated liquid)

The nominal purity of the products is:

- x_{AD} = 0.9895 molar
- x_{BS} = 0.9709 molar
- x_{CB} = 0.9815 molar

Operating conditions are not optimised. Simply, input values that fulfil the required specifications are chosen. The nominal operation is defined by:

- Reflux rate L=2.667 kmol/min
- Boilup V=3 kmol/min
- Distillate flowrate D=0.333 kmol/min
- Bottoms flowrate B=0.334 kmol/min
- Side stream flowrate S=0.333 kmol/min
- Split of liquid $SPLITD$=0.55
- Split of vapour $SPLITB$=0.5
- Holdups in all trays $M(i)$=0.5 kmol, i =2,... 29, 31,... 40.
- Holdup in reboiler and reflux drum $M(1)$=$M(30)$=10 kmol

In Figures 4.1 and 4.2, the profiles of the liquid compositions in the main column and the prefractionator are shown.

To illustrate the effect of the liquid dynamics for different reboiler and reflux drum sizes, the behaviour of the DWC with tanks of two different sizes has been simulated. A disturbance of 20% in the feed flowrate has been applied at minute 5. The column is stabilised in the following way: condenser level is controlled by D and reboiler level is controlled by B. Composition is not controlled. In Figure 4.3, the profiles of the three product compositions are plotted. For tank holdups 20 times the holdups in the regular trays (red lines), responses are clearly slower than for tank holdups equal to the regular trays holdups (green lines). About 50 minutes of difference can

be observed in the worst case. The importance of choosing realistic values for the reboiler and reflux drum holdups is apparent. Values of 20 times the regular tray holdups are realistic. Because of that, in the examples studied in this thesis work, these values are chosen. In Figure 4.3, it can also be seen that no delay is manifested: compositions begin to change at minute 5.

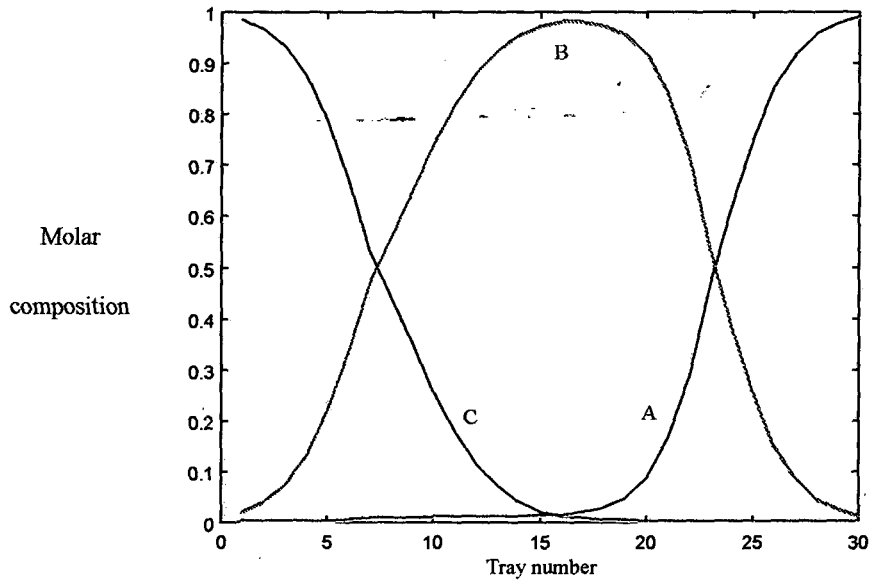

Figure 4.1: Liquid composition profiles in the main column

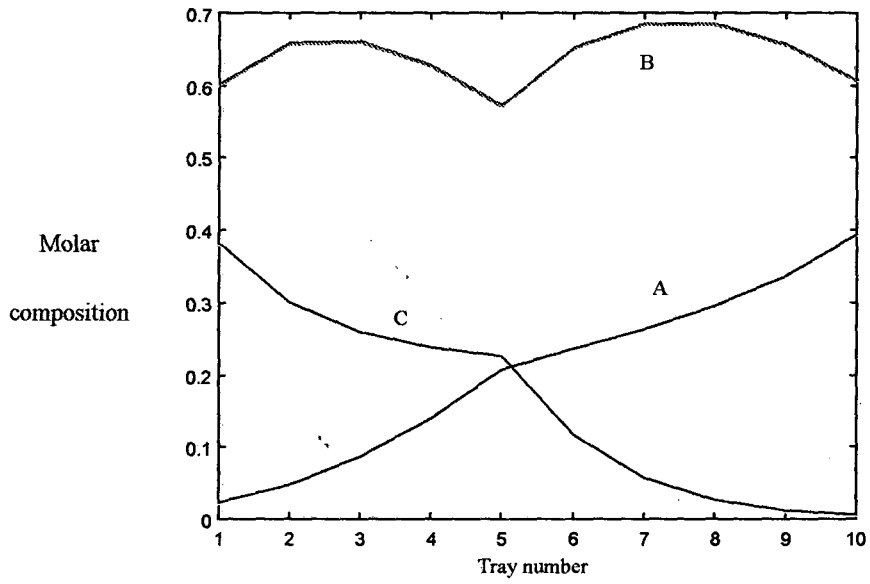

Figure 4.2: Liquid composition profiles in the prefractionator

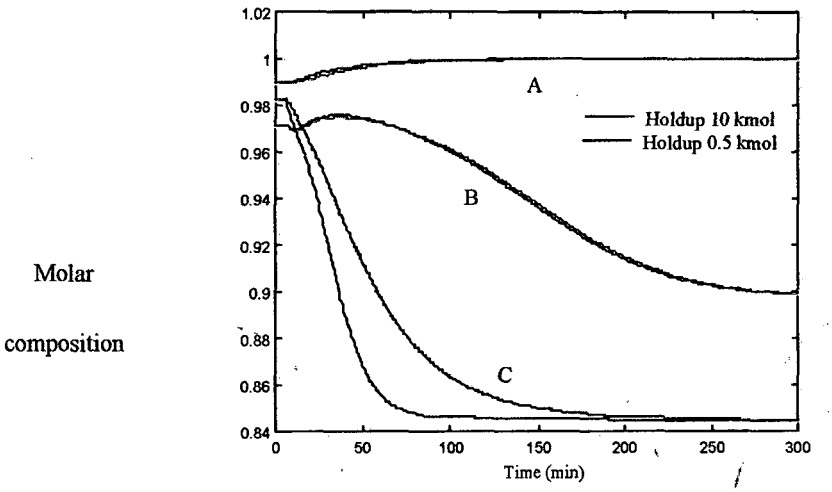

Figure 4.3: Product compositions for different tank sizes

To illustrate the effect of τ, the behaviour of the DWC model with two different τ values is simulated. The values are τ=0.063 min and τ=0.63 min. The column is also stabilised by D and B and composition control loops are open. A step disturbance of +10% in F is applied. In Figure 4.4, the tank level profiles can be seen. From the reboiler liquid level profiles, a slower response can be seen for the large τ case (blue line). The level in the condenser (cyan lines) has not changed in any case because the disturbance is an increase of liquid feed flowrate and no effect of the disturbance arrives at the condenser because it is absorbed by the reboiler. In Figure 4.5, the compositions of all three products are plotted and it is seen that the slower responses correspond always to τ=0.63 min. Therefore, the effect of τ is quite important and thus, accurate values may be required to have a proper control study. A value of τ=0.063 min will be assumed all over this thesis work. This is the value proposed by Skogestad et al. (1996).

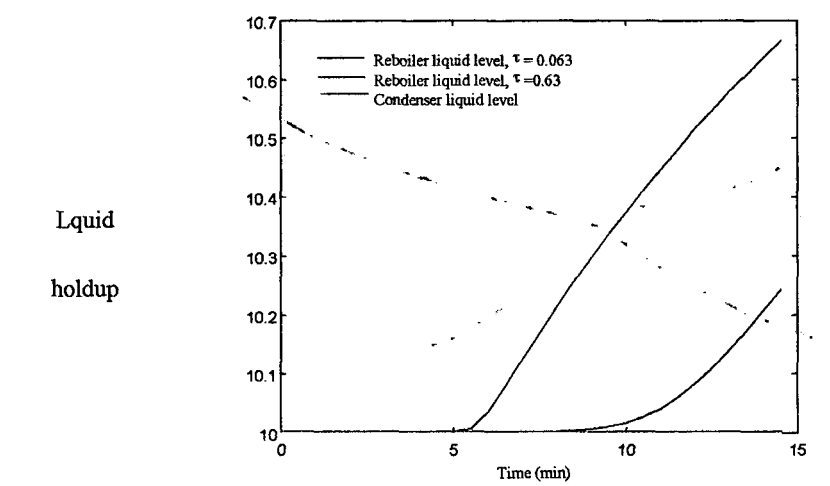

Figure 4.4: Reboiler and condenser liquid levels for different τ

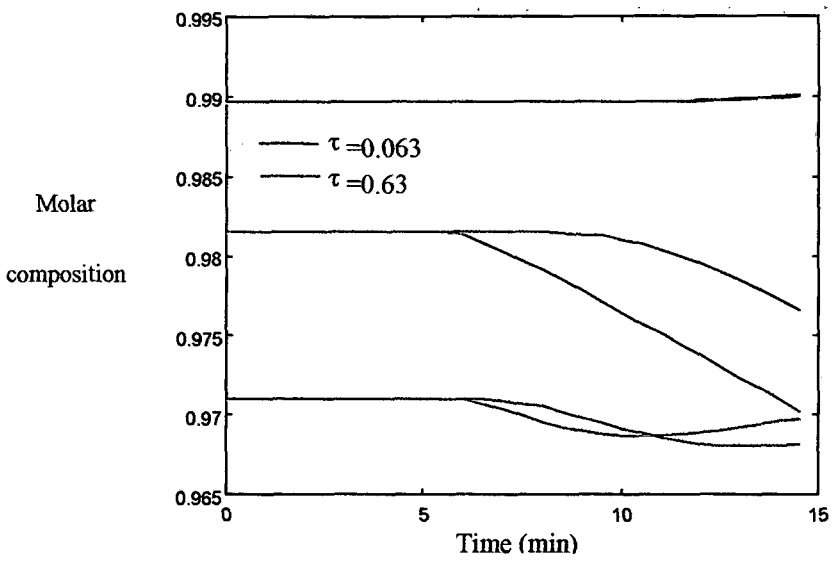

Figure 4.5: Product compositions for different τ

4.3.2 The linear model

The literature theory developed for MIMO linear systems provides with very useful tools for the stability, robustness and controllability analysis. Therefore, having a linear model of the DWC will be very useful whenever the behaviour of the linear model can be extrapolated to the non-linear real conditions. Distillation columns are known to be very non-linear. The effect of changes in the inputs depends strongly on the magnitude of the changes and the operating point. As multivariable systems, interaction between inputs is also an important aspect of the non-linearity of a distillation column. Given the non-linearity of distillation columns, especially when high purity is required, will the results obtained with the linear model apply the non-linear reality? A large amount of practical experience shows that in many cases, linear controllers designed using linear methods provide satisfactory performance when applied to real non-linear plants (Skogestad et al. 1996). The Morari approach (Morari et al., 1989) also bases the controller design on a linear model.

A large profit of DWC liner models has been taken in this work. Linear methods are used to design diagonal feedback controllers for the DWC. However, non-linear model simulations are also used to analyse the behaviour of the controllers.

4.3.2.1 The linearised system

The DWC linear models are obtained from linearisation of the non-linear model described in 4.3.1.2. The linearised systems have the inventory control loops closed. The linear models will be used to study the composition control. Therefore, the composition control analysis is done for a specific inventory control, the structure and tuning of which have been solved previously.

In the case of closing the inventory control loops with L and V, the system is unstable at steady state. As will be seen, this poses some limitations to the linearisation.

4.3.2.2 Linear model representations

Two representations of the linear models are common in the literature. One is the state-space model representation through the $\boldsymbol{A}$, $\boldsymbol{B}$, $\boldsymbol{C}$ and $\boldsymbol{D}$ matrixes. The meaning of these matrixes can be seen in equations 4.10 and 4.11, where x are the state variables, y the output variables and u the input variables.

$$dx/dt=\boldsymbol{A}x+\boldsymbol{B}u \qquad (4.10)$$

$$y=\boldsymbol{C}x+\boldsymbol{D}u \qquad (4.11)$$

The second representation is the transfer function matrix $\boldsymbol{G}$. The dimension of $\boldsymbol{G}$ is number of inputs per number of outputs. Each one of the elements of the matrix is defined as seen in equation 4.12, where the functions $y(s)$ and $u(s)$ are the Laplace transforms of $y(t)$ and $u(t)$, being t the time.

$$G(s)=y(s)/u(s) \qquad (4.12)$$

The elements of the transfer function matrix have an important property. After sending a sinusoidal signal of frequency w to the system element represented by $G(s)$, the signal's magnitude is amplified by a factor of $|G(jw)|$ and the phase is shifted by the angle defined by the complex $G(jw)$. The analysis of $\boldsymbol{G}(s)$ is known as the frequency analysis (Luyben, 1990), (Skogestad, 1996). It will be better explained in section 4.7.2.

Transfer function matrix can be calculated from $\boldsymbol{A}$, $\boldsymbol{B}$, $\boldsymbol{C}$ and $\boldsymbol{D}$ as indicated in equation 4.13, where $\boldsymbol{I}$ is the unity matrix.

$$\boldsymbol{G}(s)=[\boldsymbol{C}(s\boldsymbol{I}-\boldsymbol{A})^{-1}\boldsymbol{B}] \qquad (4.13)$$

In this work, MATLAB "Linear Time Invariant" state space and transfer function representations have been used.

4.3.2.3 Two different ways of obtaining the linear model

Two different ways of obtaining the DWC linear model from the non-linear model have been considered. One is identification by input step changes and the other is the numerical linearisation using the model of differential equations. Linearisation is done at nominal operation point.

Identification by input step changes

The most direct way of obtaining an empirical linear dynamic model of an open-loop process is to find the parameters that fit the experimentally obtained step response data (Luyben, 1990). Specifically, step response data is obtained by applying a step input change to each input at a

time and registering the response of all outputs until a new steady state is reached. The transfer function in 4.14, a transfer function of first order plus delay, is normally assumed for each input-output pair, where K is the ratio between the final steady state output increment over the input increment, τ_p is the time it takes the output to reach 63% of its final value, and d is the time it takes the output to start changing. This method do not provide a precise high order model and is quite sensitive to non-linearity.

$$G(s)=K*(e^{-ds}/(\tau_p*s+1)) \qquad (4.14)$$

Non-linearity would not be a problem if step changes in the inputs were small enough to be in the linear area. To illustrate the non-linearity of the DWC through the example in 4.3.1, its transfer function is searched using the identification method. Matrixes in 4.15 and 4.16 are the transfer functions ***G(s)*** obtained with input steps of 0.5%. ***G(s)*** in 4.15 is obtained with positive steps and ***G(s)*** in 4.16 is obtained with negative steps. The elements of the matrixes are ordered in a way that columns are the inputs (L, S and V) and rows are the outputs (product purities).

$$\begin{matrix} & L & S & V & \\ \boldsymbol{G(s)} = & \begin{pmatrix} \frac{2.06}{1+80s} & \frac{0.02}{} & \frac{-8.08}{1+105.5s} \\ \frac{-3.71}{1+352s} & \frac{-0.55}{1+85.5s} & \frac{-6.67}{1+81.5s} \\ \frac{-5.39}{1+81s} & \frac{0.41}{1+79s} & \frac{1.91}{1+37s} \end{pmatrix} & \begin{matrix} x_{AD} \\ x_{BS} \\ x_{CB} \end{matrix} \end{matrix} \qquad (4.15)$$

$$\begin{matrix} & L & S & V & \\ \boldsymbol{G(s)} = & \begin{pmatrix} \frac{7.32}{1+113s} & \frac{0}{} & \frac{-2}{1+70s} \\ \frac{-5.86}{1+84s} & \frac{-0.5}{1+81s} & \frac{4.65}{1+334s} \\ \frac{-1.84}{1+42s} & \frac{0.49}{1+85.5s} & \frac{6.17\cdot}{1+76.5s} \end{pmatrix} & \begin{matrix} x_{AD} \\ x_{BS} \\ x_{CB} \end{matrix} \end{matrix} \qquad (4.16)$$

The transfer functions obtained for positive and negative input step changes are very different, even with small step changes (a step of 0.5% is already small to be adjusted in a real plant), indicating a large non-linearity. Gain values vary more than three times from one matrix to the other. However, more important from a control point of view is that not all gain signs are equal. Therefore, none of the matrixes are appropriate linear models because the linearisation was done out of the linear area. It can be concluded that the DWC is too non-linear for the identification method to be used in a real plant. However, if an analytical model is available, steps can be made as small as necessary and the method used trough simulation.

Looking closely to the matrixes, from the steady state gain, it can be seen that:

- if the boilup is increased over its nominal value, the decrease in the purity of A in the distillate is large compared to the increase in purity of C in the bottoms product
- if the reflux is increased over its nominal value, the decrease in the purity of C in the bottoms product is large compared to the increase in the purity of A in the distillate product
- on the other hand, if the reflux is decreased below its nominal value, the decrease in the purity of A in the distillate is large compared to the increase in the purity of C in the bottoms product
- and finally, if the boilup is decreased below its nominal value, the decrease in the purity of C in the bottoms product is large compared to the increase in the purity of A in the distillate.

According to these results, increasing the purity of products is more difficult than decreasing them. This is one of the main effects of non-linearity. This behaviour is not caused by the special design of the DWC but by the high purity distillation nature.

If attention is turned to S and x_{BS} variables, that is, to the second row and second column of the matrixes, it is seen that:

- steady state gain for positive and negative changes in S are similar; a 0.5% change in S is in the linear region.
- the sign of the (2,3) element in the two matrixes is different. This element corresponds to the effect of V on x_{BS}. x_{BS} decreases either if V increases or decreases. This indicates that purity of B has a maximum for some V between V nominal + 0.5% and V nominal - 0.5%.

Numerical linearisation using the model of differential equations

This will be the method used in this work to obtain the linear models of the studied separations. With this method $\boldsymbol{A}$, $\boldsymbol{B}$, $\boldsymbol{C}$, and $\boldsymbol{D}$ matrixes are found. Taylor expansion of order one in terms of deviation variables is applied to $\boldsymbol{A}$, $\boldsymbol{B}$, $\boldsymbol{C}$, and $\boldsymbol{D}$ as seen in equation 4.17. (See equations 4.10 and 4.11, too).

$$A_{ij} = \Delta(dx_i/dt) / \Delta x_j \qquad B_{ij} = \Delta(dx_i/dt) / \Delta u_j \qquad C_{ij} = \Delta y_i / \Delta x_j \qquad D_{ij} = \Delta y_i / \Delta u_j \tag{4.17}$$

Having $3*NT$ states, very large matrixes are obtained. Specially, $\boldsymbol{A}$ is a $3NT$x$3NT$ matrix. Reduced models have been used for some applications. Balanced residualisation has been applied for the model reduction. For the separation example, 16 states have been left because it is seen that with a 16-state model, the difference between the reduced and the 120-state original model is only noticed at high frequencies (1000 rad/min).

Comparison between the two linearisation methods

With steps of the same size, 10^{-10} kmol/min, the two linearisation methods are compared. In 4.18 and 4.19, $\boldsymbol{G(0)}$ obtained with step identification and $\boldsymbol{G(0)}$ obtained with numerical linearisation

are shown. Results are practically the same indicating that the two methods give equivalent linear models at steady state. At small frequencies, the two methods also give quite similar results despite the very different s dependency (the s dependency of the linear model obtained by numerical linearisation is a polynomial of order 120 and of the transfer function assumed in the case of step identification is of order one). However, for large frequencies the differences increase. This effect can be seen in Figure 4.6, where the singular values of $G(s)$ for $L\ V\ S$ inputs and inventory control made by D and B are plot. Singular values are different for the step identification (red lines) and the numerical linearisation (blue lines) at large frequencies. Since high frequencies are not relevant in distillation control analysis, non-precise high order models given by step identification method could be appropriate. However, differences between the two models are already found for frequencies of 0.02 rad/min, and this is still in the range of frequencies of importance for the distillation columns, as will be seen in 4.7.2. Therefore, the linearised model found with numerical linearisation will give more precise results.

$$G(0) = \begin{array}{c} \begin{matrix} L & V & S & SPLITD & SPLITB \end{matrix} \\ \begin{pmatrix} 1.26 & -1.41 & 0.002 & 0.008 & -0.01 \\ 0.58 & -0.64 & -0.10 & 0.02 & -0.02 \\ -0.68 & 0.78 & 0.08 & 0.02 & -0.01 \end{pmatrix} \end{array} \begin{matrix} x_{AD} \\ x_{BS} \\ x_{CB} \end{matrix} \qquad (4.18)$$

$$G(0) = \begin{array}{c} \begin{matrix} L & V & S & SPLITD & SPLITB \end{matrix} \\ \begin{pmatrix} 1.28 & -1.43 & 0.002 & 0.008 & -0.01 \\ 0.58 & -0.64 & -0.10 & 0.02 & -0.02 \\ -0.68 & 0.78 & 0.08 & 0.02 & -0.01 \end{pmatrix} \end{array} \begin{matrix} x_{AD} \\ x_{BS} \\ x_{CB} \end{matrix} \qquad (4.19)$$

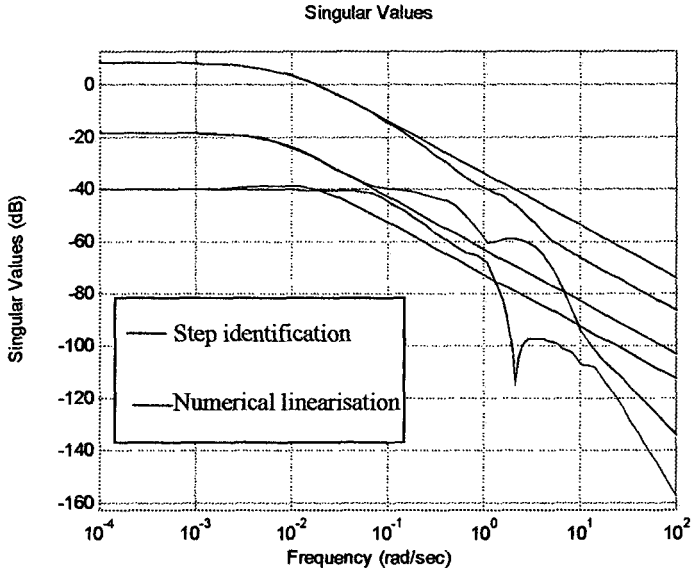

Figure 4.6: Singular values of $G(s)$

Comparing the two linearisation methods, it has to be said that the identification method can be only used to linearise open loop stable systems because the new steady state output values are required. For this reason, it can not linearise the DWC with inventory control made by L and V, which it is not stable. However, equation 4.17 can still be used to obtain the state-space matrixes for a DWC with inventory control made by L and V. To avoid having results corresponding to the column at strange operation conditions, values at small frequencies have not been taken into account.

4.3.2.4 Scaling

A useful approach for scaling, proposed by Skogestad (1996), is to make the variables less than one in magnitude. This is the approach in this work. It requires the engineer to make a judgement at the start of the design process about the required performance of the system. The scaling approach consists in dividing each variable by its maximum expected or allowed change. For disturbances and manipulated variables, the scaling is:

$$d_{scaled}=d_{unscaled}/d_{max} \qquad u_{scaled}=u_{unscaled}/u_{max} \qquad (4.20)$$

where d are disturbances, u are inputs, d_{max} are the largest expected disturbance changes, and u_{max} are the largest allowed input changes. The scaling of the outputs can be done for the largest allowed control error or the largest expected change in reference value. In this work, the first option is taken:

$$y_{scaled}=y_{unscaled}/y_{max} \qquad (4.21)$$

where y are outputs and y_{max} are the largest allowed output errors.

In this work, d_{max} and u_{max} have been assumed the 20% of the d and u corresponding variables. Since the considered outputs will be all product compositions, y_{max} is assumed to be 0.01 molar fraction.

Scaling is very important in practical applications as it makes model analysis and controller design much simpler. Two of the most important parameters used to study control performance are the Morari Resiliency Index (*MRI*) and Condition Number (*CN*), which derive form the singular value decomposition of the transfer function. Singular values depend on the scaling. Also the Closed Loop Disturbance Gain (***CLDG***) and the Performance Relative Gain Array (***PRGA***), two matrixes used for the controllability study, are scaling dependent. Another controllability index used is the Relative Gain Array (***RGA***). The elements of the ***RGA*** matrix on the contrary, are adimensional and do not depend on the scaling. In section 4.7.3, the definition of these controllability indexes will be given.

4.4 Two operating conditions

In order to have two examples for the next sections of this chapter, a second example is introduced. In this case, the column design is the same than the one of the example in section 4.3.1.2. Also the same separation problem is considered. However, different operating conditions are considered. The nominal operation of the example in section 4.3.1.2 was not optimal. Contrarily, the example described in this section has optimal nominal operation. Specifying the purity of the three products, the steady state with minimum boilup has been searched. In chapter six, more details on the used DWC optimisation procedure will be given. The optimal nominal operation found is described next.

- Reflux rate L=1.944 kmol/min
- Boilup V=2.276 kmol/min
- Distillate flowrate D=0.332 kmol/min
- Bottoms flowrate B=0.335 kmol/min
- Side stream flowrate S=0.333 kmol/min
- Split of liquid $SPLITD$=0.639
- Split of vapour $SPLITB$=0.477
- Holdups in all trays M(i)=0.5 kmol, i = 2,... 29, 31,... 40
- Holdup in reboiler and reflux drum $M(1)$=$M(30)$=10 kmol

The boilup flowrate of the optimal nominal operation is 25% lower than the boilup flowrate of the non-optimal nominal operation. The composition profiles for the optimal operating conditions are shown in Figures 4.7 and 4.8.

Comparing Figures 4.1, 4.2 with Figures 4.7, and 4.8, the most remarkable difference between the composition profiles of the two examples is the symmetry presented by the B composition in the main column and in the prefractionator for the separation at optimal operation.

The process has also been optimised leaving the feed vapour fraction free, and the minimum boilup has been found for q_F=0 (saturated vapour feed). Decreasing q_F (increasing feed vapour fraction), the minimum boilup is lower and the reflux is higher. As seen above, for q_F=1 (saturated liquid feed), L=1.94 kmol/min and V=2.27 kmol/min. For q_F=0 (saturated vapour feed), L=2.46 kmol/min and V=1.79 kmol/min. The difference in boilup requirement is really large, 27%. As indicated in section 2.5.4, it is important to consider the vaporisation of the feed before entering the DWC. However, because a decrease in the boilup will implicate an increase in the reflux, the best feed heat condition will depend on the disposability of cold and hot streams in the plant.

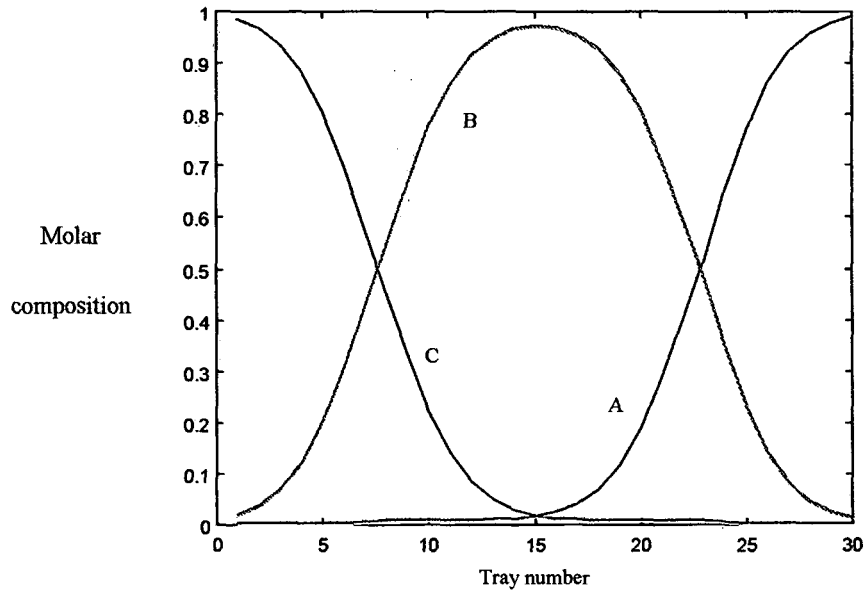

Figure 4.7: Composition profiles in the main column

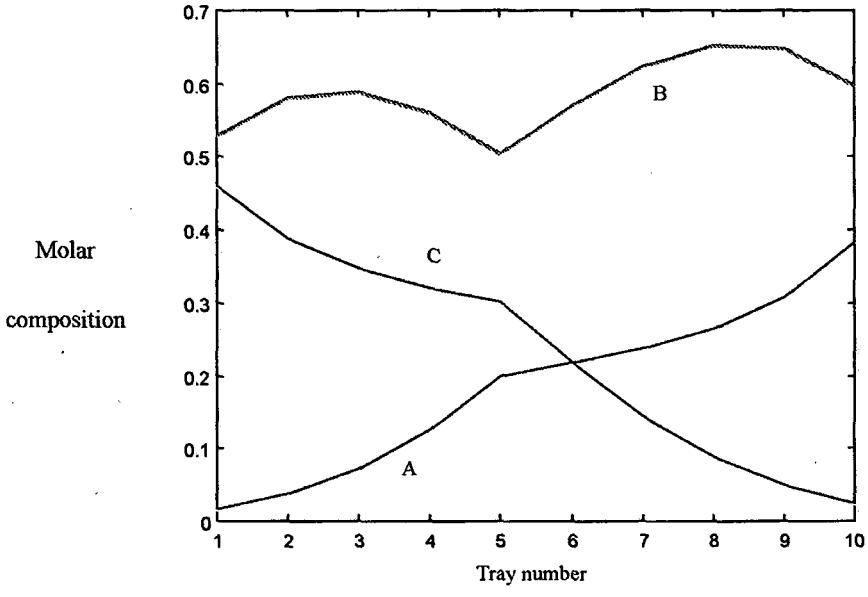

Figure 4.8: Composition profiles in the prefractionator

4.5 Degrees of freedom and control levels

Because of the large difference between the mass flow dynamics time constants and the composition dynamics time constants, many authors propose to solve the control problem of

distillation columns by levels (Luyben, 1992). The lower level is the stabilisation of the process, the inventory control. The upper level is the separation control or composition control. Finally, if extra degrees of freedom are available, another control level can be added, the optimising control.

The approach proposed in the last paragraph is adequate for the DWC and will be the approach followed to analyse the control of the DWC in this thesis work. Since pressure is not considered in the proposed DWC model, the inventory control reduces to the control of the tank liquid levels. As indicated, the inventory control will be solved first. Then, the separation control will be studied over the stabilised DWC. Different inventory control structures will be proposed and for each of them, the analysis of the composition control will be developed. Finally, optimisation control will be considered.

According to the model described, the DWC has seven operation DOF, corresponding to seven candidate manipulated variables in the process. They are the *L*, *V*, *S*, *D*, *B*, *PLITD*, and *SPLITB*. Of the seven DOF, two will be used to stabilise the column, and three will be used to control the product compositions. The two remaining operation DOF can be used for optimising control.

In this work, the three operation DOF used for composition control will be specifically used for the control of the A molar fraction in the distillate, the B molar fraction in the sidestream product, and the C molar fraction in the bottoms product.

4.6 Inventory control

Typically, when considering a column in isolation, the level in the reflux drum is controlled manipulating the distillate flowrate and the level in the reboiler is controlled manipulating the bottoms flowrate. This type of control scheme would be used for a column with low to moderate reflux ratios (less than 4) (Lyuben et al., 1998). However, when a large flow and a small flow leave a tank, the large has to be used to control the tank liquid level. Therefore, for columns with high reflux ratios (reflux much larger than distillate), the control of the reflux drum level should be done manipulating the reflux, not the distillate. Of course, similar arguments apply to the reboiler level control in columns where the boilup is much larger than the bottoms flowrate.

According to this, in a DWC, the use of *D* and *B* to control the liquid level in the reboiler and reflux drum is not encouraged because typically, the DWC has large reflux ratios (larger than 4) at both extremes. For the separation example at optimal operating conditions, L/D=5.8 and V/B=6.8. For optimal designs of the DWC found in the literature, reflux ratios are never lower than 4 for moderate purity requirements (about 0.95). Because of that, in this work, special attention is given to the inventory control configuration in what the manipulated variables are *L* (for the condenser level) and the *V* (for the reboiler level).

This inventory control configuration has the particularity that both manipulated variables are internal streams. Because of that, with the composition control loops open, changes in external variables unstabilise the system and the gain matrix is singular at steady state. For this reason, for simple columns, the inventory control structure was not considered by most distillation control experts. However, it was shown that the configuration does actually work (Skogestad et al., 1990 a).

In this work, the following structures for stabilisation control are considered:

- "DB" stabilisation: control of the level in the condenser by the distillate flowrate, control of the level in the reboiler by the bottoms flowrate
- "LB" stabilisation: control of the level in the condenser by the reflux flowrate, control of the level in the reboiler by the bottoms flowrate
- "DV" stabilisation: control of the level in the condenser by the distillate flowrate, control of the level in the reboiler by the boilup
- "LV" stabilisation: control of the level in the condenser by the reflux flowrate, control of the level in the reboiler by the boilup

For each of these possible inventory control structures, the search for the best composition control structures will be done.

4.6.1 Controllers of the inventory control loops

As explained by Luyben (1990), in real plants, most liquid levels represent material inventory used as surge capacity. In these cases, it is unimportant where the level is, as long as it is between some maximum and minimum values: "If PI controllers are used to held the level right at its setpoint we might as well not even use a tank!". Because of that, proportional controllers are often used to control liquid levels, in order to give smooth changes and filter out fluctuations in flowrates affecting downstream units.

In distillation columns, the reboiler and reflux drum are large enough to absorb fluctuations. Because of that, in this work, proportional controllers have been implemented in both inventory control loops.

For both described examples, the holdup in the reflux drum and the holdup in the reboiler are 20 times the holdup in the regular trays. Tanks of double capacity than the holdup volumes are assumed (such tanks are large enough to maintain the liquid levels between reasonable maximum and minimum values). The tuning of the proportional controllers has been done in such a way that the control valve is half open when the tank is half full (nominal values), the control valve is wide open when the tank is 75% full, and the control valve is closed when the tank is 25% full. The saturation of the valve is supposed at a flowrate double than the nominal flowrate.

According to this, the tuning of the inventory controllers for both examples are found. Non scaled values are shown in Table 4.1 for each one of the inventory control alternatives. Only in section 4.7.4, some different tunings are applied in order to study its effect on the composition control.

Table 4.1: Non-scaled proportional constants of the inventory controllers (non-optimal operation/optimal operation)

Inventory control	"D B"	"L B"	"D V"	"LV"
Condenser loop	0.066	0.53/0.39	0.066	0.53/0.39
Reboiler loop	0.066	0.066	0.60/0.45	0.60/0.45

4.7 Composition control

Generally, direct composition measurements will lead to better composition control than temperature measurements. Besides, temperature can be a very poor indicator of composition for multicomponent mixtures. In this work, composition measurements are considered, and sample points are located at the product streams.

Having selected the measured variables, the determination of the diagonal feedback controller consists in the selection of the manipulated variables, the pairing of the manipulated variables with the measured or controlled variables, and the tuning. Candidate manipulated variables are *L*, *V*, *D*, *B*, *S*, *SPLITD* and *SPLITB*, taking off in each case the variables used for the stabilisation.

In this chapter and the posterior ones, when the pairing of the control structure is relevant, the manipulated variables will be ordered in such a way that the first one controls the A composition, the second one controls the B composition, and the third one controls the C composition.

4.7.1 The composition controllers

The integral mode of a feedback controller is required to avoid steady state offset resulting from disturbances. It is usually combined with the proportional mode in a Proportional Integral (PI) controller. The transfer function representation of a PI controller isexpressed in 4.22, where K_c is the gain of the controller, τ_c is the time constant of the controller, and I is the integral time or reset time of the controller. I is the time required for a given input deviation to produce an equal change in output.

$$K_c*((\tau_c s+1)/(\tau_c s))=K_c+I/s \qquad (4.22)$$

In this chapter, PI controllers are the controllers implemented in the composition control loops.

4.7.2 Frequency domain analysis

The simplest interpretation of the transfer function ***G(s)*** is that it represents the system sinusoidal response. Since all signals can be decomposed as sum of sinusoids of different frequencies, it is worthy knowing the response of the system to sinusoids of different frequencies. A frequency domain analysis, in particular at frequencies around the bandwidth, is very useful for the feedback control study.

The bandwidth (w_B) is an indicator of the range of frequencies over which control is effective. The effect of disturbances is usually largest around the bandwidth frequency: slower frequencies are attenuated by the feedback control and faster disturbances are usually attenuated by the process itself. At frequencies lower than the bandwidth ($w<w_B$), feedback is effective and will affect the frequency response. At frequencies higher than the bandwidth ($w>w_B$), the response will not be affected by the feedback.

Several bandwidths can be defined depending on the interpretation of effective control. One of the more used bandwidth definitions is the frequency where the magnitude of the sensitivity function ***S*** crosses 0.707 from below for first time (Skogestad, 1996). This is the definition considered in this work. For MIMO systems, the bandwidth will depend on the direction and there is a bandwidth region between a lower frequency where the maximum singular value of ***S*** reaches 0.707 and a higher frequency where the minimum singular value of ***S*** reaches 0.707. However, to associate a single bandwidth frequency to a MIMO system, the worst case direction is considered and the bandwidth is defined as the frequency where the maximum singular value of ***S*** reaches 0.707 from below for first time.

Two functions characteristic of the control structure and depending on the frequency are usually used to compare the controllability of different candidate composition control structures. They are the singular value decomposition and the ***RGA***. For control purposes, singular value decomposition and ***RGA*** have to be analysed at frequencies around the bandwidth frequency.

Since $\boldsymbol{S}=(\boldsymbol{I}+\boldsymbol{G}^*\boldsymbol{K})^{-1}$, where ***K*** is the controller transfer function, the bandwidth will not be known until the controller structure and tuning are known. Thus, there is one problem because the frequency range where singular value decomposition and ***RGA*** have to be analysed when they are used to select the control structure is not known before the control structure and tuning are known.

The inverse of the main open-loop time constant is a characteristic frequency of the system. In distillation, the main time constants are given by the composition dynamics. High purity columns have very large open-loop time constants. However, the use of feedback changes the dynamics and the closed-loop time constants may become much shorter. The main time constant of an open-loop system can be calculated as the inverse of the eigenvalue of the state-space matrix ***A*** with smallest magnitude (Skogestad, 1996).

The main open-loop time constant will give a first idea of the range of frequencies of interest. To solve the problem of unknown bandwidth, as first approach, it will be considered that the closed-loop time constant is about 10 times smaller than the open-loop time constant. Thus, as first approach, it will be considered that the frequencies of interest are about 10 times the frequency corresponding to the main open loop time constant.

For the studied separations, the A eigenvalues with smallest magnitude of the stable systems are -0.004 for the non-optimal operation case, and –0.006 for the optimal operation case. Thus, in the frequency dependent analysis, special attention will be given to the values around 0.04 rad/min and 0.06 rad/min. In the case of "LV" inventory control, the A eigenvalue with smallest magnitude is 0. This is because of the instability. However, the following eigenvalues with smallest magnitude are -0.004 and -0.006. In the frequency dependent analysis, special attention is also given to values around 0.04 rad /min and 0.06 rad/min.

Skogestad et al. (1990 a) stated that the frequency range important for feedback control is the frequency range from about 0.01 to 1 min^{-1}. This gives another idea of the range of frequencies of interest.

4.7.3 Linear analysis tools

The singular value decomposition of the transfer function ***G(s)*** will be used to select the manipulated variables for the composition control. For MIMO systems, interaction between control loops as well as loop sensitivity affect the control system behaviour. The singular value decomposition is a numerical algorithm useful in analysing the multivariable aspect of the gain matrix, giving the input and output directions for which gains are maximum and minimum. The *MRI* is the smallest singular value of the open-loop transfer function. It is the poorer gain of the process, poorer sensitivity, which corresponds to specific input and output directions. The set of manipulated variables that gives the largest *MRI* over the frequency range of interest is preferred.

Another index derives from the singular value decomposition of ***G(s)***. It is the ratio of the maximum singular value to the minimum singular value or *CN*, a typical index for the selection of the best set of manipulated variables. It provides a numerical indication of the sensitivity balance in a multivariable system. Large condition numbers indicate unbalanced sensitivity and also sensitivity to changes in process parameters. Therefore, the sets of manipulated variables with smaller *CN* are preferred. Skogestad (1996) explained that *CN* larger than 10 may indicate control problems.

RGA is used to determine the interaction among control loops in a multivariable process and it is frequently used to select the control pairing. It is defined as the ratio of the open-loop gain for a selected output when all loops on the process are open, to its open-loop gain when all the other loops are closed. ***RGA*** of a complex non-singular matrix A is calculated as indicated in equation 4.23, where X denotes element by element multiplication.

$$RGA(A)=AX(A^{-1})^{T} \qquad (4.23)$$

Pairings that have ***RGA*** close to unity matrix at frequencies around the bandwidth are preferred. This rule favours minimal interaction between loops, which means independence of the loops. Being the loops independent, stability problems caused by interaction are prevented. Numbers around 0.5 indicate interaction. The ***RGA*** indicates other useful control properties (Skogestad et al., 1996). One of the most important, plants with large ***RGA*** elements around the bandwidth frequency are difficult to control because of sensitivity to input uncertainty.

Another rule to pair control variables is to choose pairings of variables that are close to each other. These pairings will put minimal restrictions to the achievable bandwidth, which should be as large as possible.

Two other matrixes have been used for the study of the DWC diagonal feedback control, the ***CLDG*** and the ***PRGA***. Their expressions can be seen in equations 4.24 and 4.25, where ***Gdiag*** is a diagonal matrix with the diagonal elements of ***G***, and ***Gd*** is the transfer function corresponding to the disturbances.

$$PRGA=Gdiag*G^{-1} \qquad (4.24)$$

$$CLDG= Gdiag*G^{-1}*Gd \qquad (4.25)$$

$|Li|$ larger than $|PRGA(i,j)|$ and $|CLDG(i,j)|$ per all j are required for acceptable disturbance rejection and setpoint tracking performance. $|Li|=|G(i,i)*Ki|$, where Ki is the transfer function of the controller in loop i. Therefore, the disturbances and setpoint changes corresponding to large ***CLDG*** and ***PRGA*** elements will be more difficult to control. This way, the elements of ***CLDG*** and ***PRGA*** inform of which of the disturbances (***CLDG***) and setpoint changes (***PRGA***) require larger bandwidths and larger controller gains for acceptable performance (Skogestad, 1997). In the case of the ***PRGA*** elements, $|Li|$ larger than $|PRGA(i,j)|$ is only required at frequencies where setpoints are tracked.

4.7.4 Search of the set of manipulated variables and the pairing

In this section, the best composition control structures for the separation example at optimal and non-optimal operating conditions are searched. To determine the control structure, the set of manipulated variables has to be determined, as well as the pairing between manipulated variables and controlled variables. *MRI* and *CN* are used to select the set of manipulated variables. Sets with large *MRI* (large sensitivity in the worst direction) and small *CN* (balanced sensitivities in different directions) are preferred. ***RGA*** is the criterion used to select the pairing. Pairings with ***RGA*** closer to unity (smaller interaction between loops) are preferred.

As explained in section 4.7.2, frequencies around 0.04 rad/min for the non-optimal example and around 0.06 rad/min for the optimal example are given special importance.

4.7.4.1 Composition control structure for "DB" inventory control

In this section, the best composition control structure for the DWC with "DB" stabilisation is searched. The separation example at non-optimal operation is analysed first, followed by the analysis of the separation example at optimal operation.

Non-optimal operation

- *Set of manipulated variables:*

The best five sets of manipulated variables in terms of *MRI* and *CN* are shown in Table 4.2. Values at steady state ($s=0$) and at 0.04 rad/min ($s=0.04$) are indicated. The results show that the split variables (*SPLITD and SPLITB*) are good manipulated variables. The *CN* are quite large (ill conditioning), indicating unbalanced multivariable gains.

Table 4.2: Controllability parameters of the best sets of manipulated variables

Set of manipulated variables	*MRI*		*CN*	
	$s = 0.04$	$s = 0$	$s = 0.04$	$s = 0$
L S SPLITD	1.44	3.0	20	51
L S SPLITB	1.44	2.7	20	58
V S SPLITD	1.43	3.0	23	57
V S SPLITB	1.43	2.7	23	65
L V S	0.87	0.9	51	260

Comparing the singular values of the *L S SPLITD*, *L S SPLITB*, *V S SPLITD*, and *V S SPLITB* structures, it is seen that they are very similar all over the range of frequencies. Plots are shown in Figure 4.9. However, of the 4 preferred structures, the ones including *SPLITB* will not be preferred because in practice, *SPLITB* will be more difficult to manipulate than *SPLITD*. On the other hand, similar responses are expected with *L S SPLITD* and *V S SPLITD* control structures.

To see what is the influence of the tuning of the inventory control loops on the structure selection, the singular value decomposition analysis is repeated changing it. Neither at steady-state nor for s=0.04, the results of the singular value decomposition have changed. Even with perfect control in the tanks, no difference has been found in the singular value decomposition results. For simple columns, Skogestad (1997) already explained that the tuning of "DB" inventory control does not influence the composition control.

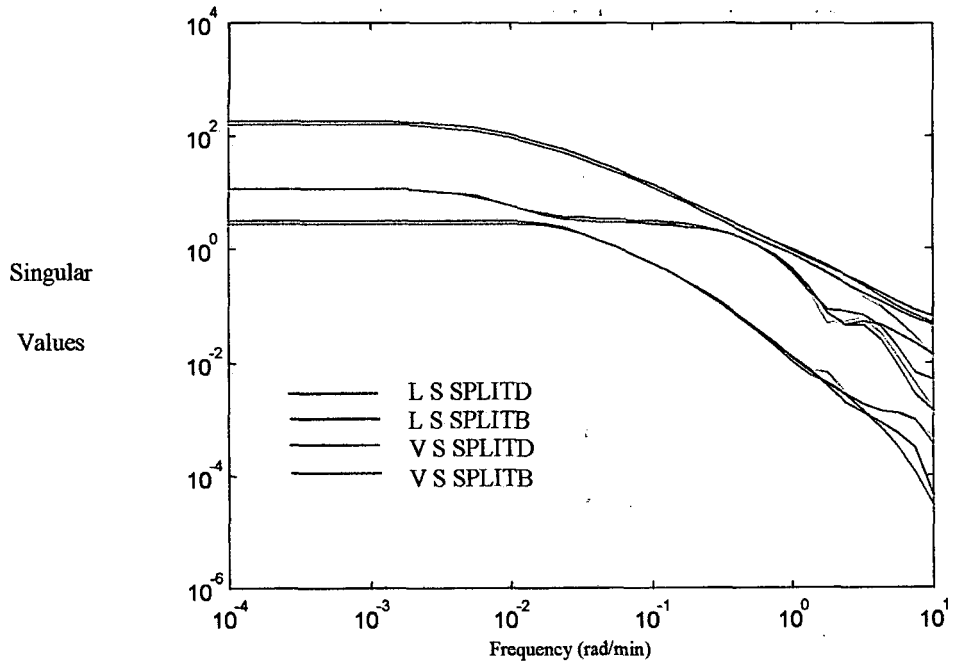

Figure 9: *L S SPLITD, L S SPLITB, V S SPLITD, V S SPLITB* singular values

- *Pairing:*

The steady state ***RGA*** for the *L S SPLITD* control structure can be seen in 4.27. It is seen that the subsystem of *S* and *SPLITD* controlling x_{BS} and x_{CB} has important interaction.

$$\boldsymbol{RGA}(0) = \begin{array}{c} \begin{matrix} L & S & SPLITD \end{matrix} \\ \begin{pmatrix} 0.962 & 0.009 & 0.028 \\ -0.071 & 0.533 & 0.538 \\ 0.109 & 0.458 & 0.433 \end{pmatrix} \end{array} \begin{matrix} x_{AD} \\ x_{BS} \\ x_{CB} \end{matrix} \qquad (4.27)$$

The diagonal ***RGA*** elements for *L S SPLITD* and *L SPLITD S* paired structures are plotted in Figures 4.10 and 4.11. It can be seen that at the frequency of 0.04 rad/min the *L SPLITD S* ***RGA*** elements are closer to one than the *L S SPLITD* ones, indicating that the *L SPLITD S* pairing is better. This pairing does not fulfil the rule of pairing variables that are close in the real process because it consists in the control of B product with *SPLITD* and the control of C product with *S*.

A very similar case occurs with the *L S SPLITB* structure. ***RGA*** diagonal elements of *L SPLITB S* paired structure are closer to one than those of *L S SPLITB* paired structure at the frequency of 0.04 rad/min. This can be seen in Figures 4.12 and 4.13.

According to the performed analysis, the preferred composition control structure for the non-optimal example with "DB" inventory control is the paired structure *L SPLITD S*.

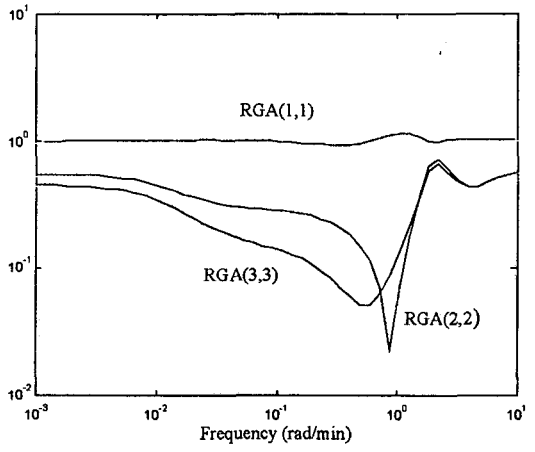

Figure 4.10: ***RGA*** diagonal elements of *L S SPLITD* paired structure

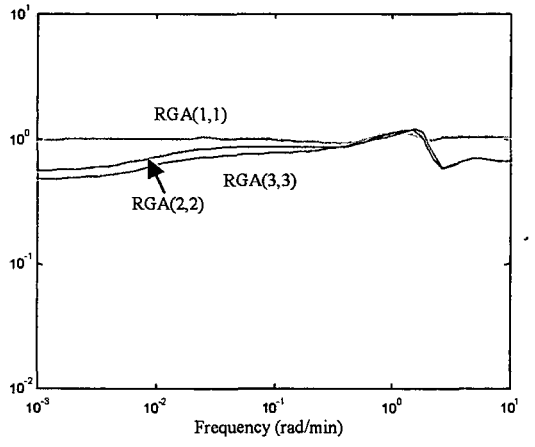

Figure 4.11: ***RGA*** diagonal elements of *L SPLITD S* paired structure

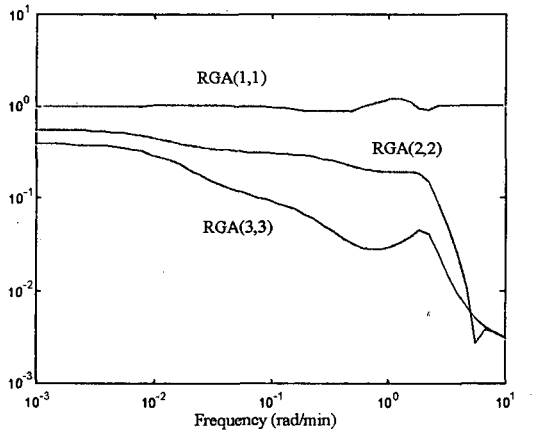

Figure 4.12: ***RGA*** diagonal elements of *L S SPLITB* paired structure

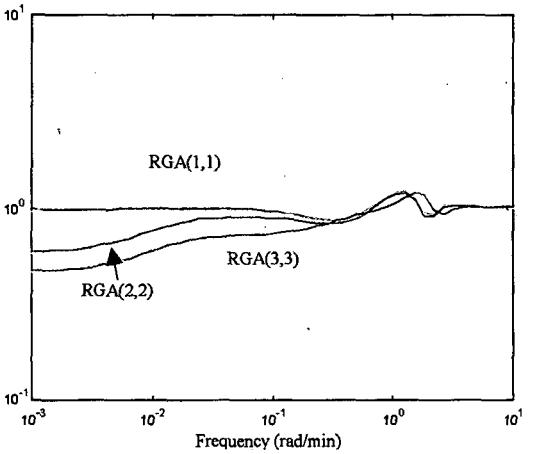

Figure 4.13: ***RGA*** diagonal elements of *L SPLITB S* paired structure

Optimal operation

- *Set of manipulated variables:*

For the optimal operation, the structures with better *MRI* and *CN* values are indicated in Table 4.3.

Table 4.3: Controllability parameters of the best sets of manipulated variables

	MRI		*CN*	
	$s = 0.06$	$s = 0$	$s = 0.06$	$s = 0$
L S SPLITD	0.18	0.22	61	425
L S SPLITB	0.17	0.21	65	436
V S SPLITD	0.18	0.22	72	491
V S SPLITB	0.17	0.22	77	505
L V S	0.55	0.60	32	236
L V SPLITD	0.25	0.005	69	29000
L V SPLITB	0.26	0.005	67	30000

It can be seen that the preferred set of manipulated variables is *L V S*. Surprisingly enough, the preferred control structures for the optimal and the non-optimal examples are different.

- *Pairing*

Looking at the ***RGA*** of the different possible paired structures with the $L\ V\ S$ set, it is found that the best pairing is $L\ S\ V$. In this case, the rule to pair variables close to each other is fulfilled. ***RGA*** diagonal elements of the $L\ S\ V$ paired structure are very high at steady state. However, they are lower at higher frequencies. As frequency increases, all three diagonal elements tend to one, as can be seen in Figure 4.14. This is because initial responses do not present interaction. The ***RGA*** matrix for $L\ S\ V$ paired structure at s=0.06 is shown in 4.28.

$$\begin{matrix} & L & S & V & \\ \boldsymbol{RGA}(0.06) = & \begin{pmatrix} 5.1 & 0.001 & 4.7 \\ 0.88 & 0.56 & 1.3 \\ 4.0 & 0.44 & 4.1 \end{pmatrix} & \begin{matrix} x_{AD} \\ x_{BS} \\ x_{CB} \end{matrix} \end{matrix} \qquad (4.28)$$

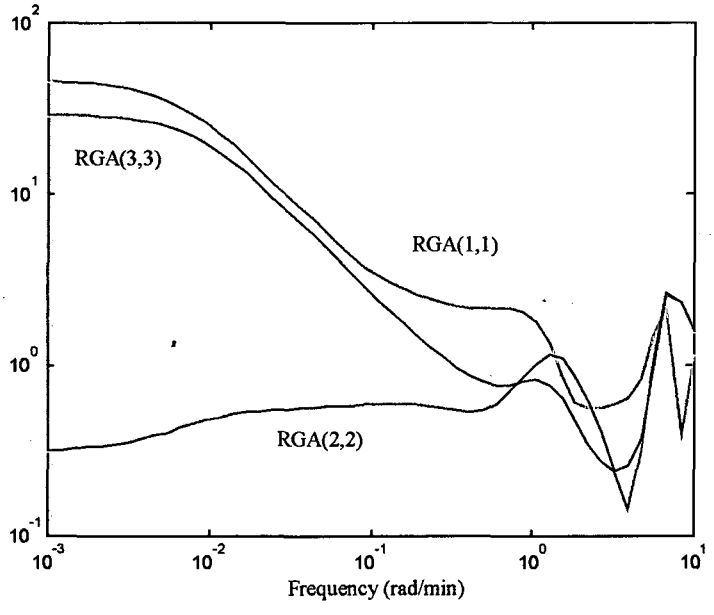

Figure 4.14: ***RGA*** diagonal elements of $L\ S\ V$ for optimal operation

Interestingly enough, the controllability indexes for the preferred control structure at optimal operation are worse than the controllability indexes for the preferred control structure at non-optimal operation: smaller *MRI*, larger *CN* and less diagonal ***RGA***. These two control structures at their corresponding operating conditions will be further studied in section 4.9.1.

4.7.4.2 Composition control structure for "LB" inventory control

Non-optimal operation

- *Set of manipulated variables:*

The three best sets of manipulated variables, according to the *MRI* and *CN* controllability indexes, for the non-optimal separation case are indicated in Table 4.4. At s=0.04, controllability indexes of the three structures are similar. However, *D S SPLITD* structure is slightly better.

Table 4.4: Controllability indexes for the best sets of manipulated variables

Structure	*MRI*		*CN*	
	s = 0.04	s = 0	s = 0.04	s = 0
D S SPLITD	1.15	3.0	5.0	7
D S SPLITB	1.16	2.7	4.9	8
V D S	0.96	1.3	6.1	15

- *Pairing:*

RGA diagonal elements for the *D S SPLITD* paired structure are plotted in Figure 4.15. For the *D SPLITD S* paired structure they are plotted in Figure 4.16. As for *L S SPLITD* and *L SPLITD S* for "DB" inventory control, *D SPLITD S* is preferred and the rule of pairing variables close to each other is not fulfilled. In fact, the ***RGA*** diagonal elements of *D S SPLITD* and *D SPLITD S* paired structures for "LB" inventory control are very similar to ***RGA*** diagonal elements of *L S SPLITD* and *L SPLITD S* paired structures for "DB" inventory control.

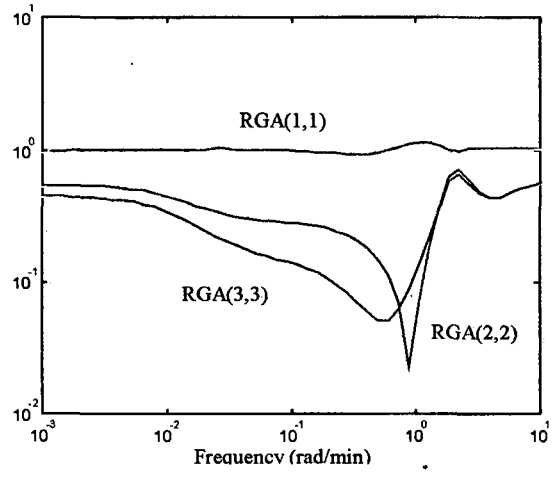

Figure 4.15: ***RGA*** diagonal elements of *D S SPLITD* structure

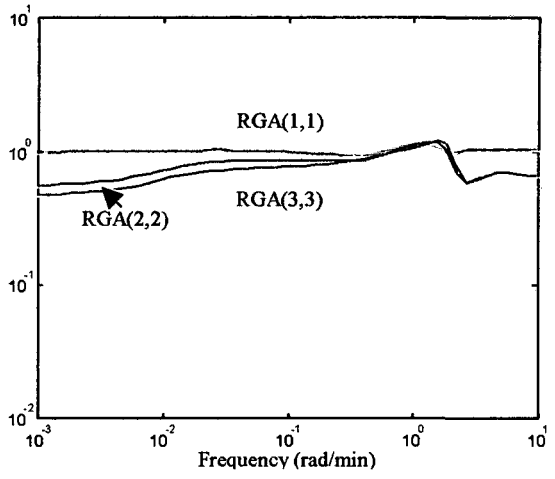

Figure 4.16: ***RGA*** diagonal elements of *D SPLITD S* structure

The singular value decomposition analysis is repeated changing the tuning of the inventory control. A proportional constant of 5 substitutes the former value 0.53 in the condenser level loop. At s=0.04, the *MRI* and *CN* indexes indicate that *V D S* structure is better than *D S SPLITD* structure. Therefore, changing the tuning of the inventory control, the preferred control structure has changed.

It has been seen that *V D S* is the preferred control structure when the inventory control is tight, whereas *D S SPLITD* is the preferred control structure when the inventory control is loose. Comparing these two scenarios, in terms of *MRI* and *CN* at s=0.04, the *V D S* control structure with tight inventory control is better. Therefore, if the inventory loop can be tight without any side problem, tight inventory control and *V D S* composition control structure will be preferred.

Optimal operation

V D S structure is found to be the best one. Its controllability indexes at s=0 are *MRI*=0.94 and *CN*=20. At s=0.06, *MRI*=0.45 and *CN*=9.

4.7.4.3 Composition control structure for "DV" inventory control

Non-optimal operation

- *Set of manipulated variables:*

The best sets of manipulated variables and their controllability indexes can be seen in Table 4.5. The *G(s)* singular values for *B S SPLITD* and *B S SPLITB* structures are very similar for all frequencies. However, as *B S SPLITD* uses *SPLITD* instead of *SPLITB*, *B S SPLITD* will be preferred.

Table 4.5: Controllability indexes for the best sets of manipulated variables

Structure	*MRI*		*CN*	
	$s = 0.04$	$s = 0$	$s = 0.04$	$s = 0$
B S SPLITD	1.36	3.0	3.6	7.8
B S SPLITB	1.35	2.7	3.5	8.9
L B S	0.87	1.2	5.7	19.7

- *Pairing:*

RGA indicates that *S SPLITD B* is the preferred paired structure with the set of manipulated variables. A matrix very close to unity indicates little interaction. The ***RGA*** at s=0.04 can bee seen in 4.29. The ***RGA*** diagonal elements can be seen in Figure 4.17.

$$\begin{matrix} & S & SPLITD & B & \\ \boldsymbol{RGA}(0.04) = & \begin{pmatrix} 0.96 & 0.04 & 0.05 \\ 0.08 & 0.85 & 0.14 \\ 0.04 & 0.15 & 0.91 \end{pmatrix} & \begin{matrix} x_{AD} \\ x_{BS} \\ x_{CB} \end{matrix} \end{matrix} \qquad (4.29)$$

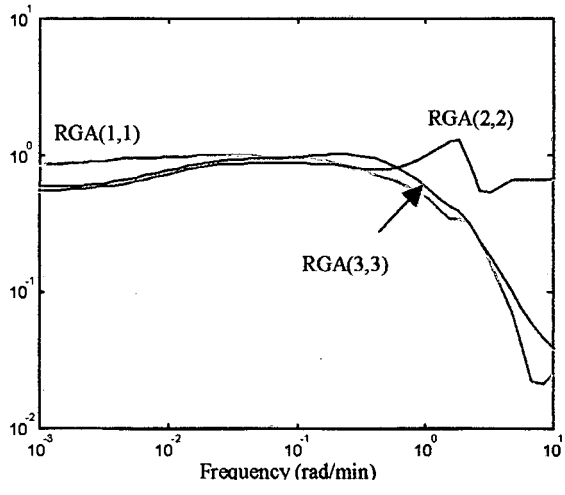

Figure 4.17: ***RGA*** diagonal elements of *S SPLITD B* structure

Optimal operation

The preferred control structure for optimal operation is *L B S*. Its controllability indexes at s=0 are *MRI*=0.8 and *CN*=23. At s=0.06, *MRI*=0.56 and *CN*=4.8.

4.7.4.4 Composition control structure for "LV" inventory control

Non-optimal operation

- *Set of manipulated variables:*

In Table 4.6, the controllability indexes of the best sets of manipulated variables are shown. They indicate that the preferred control structure is *D B S*.

Table 4.6: Controllability indexes for the best sets of manipulated variables.

	MRI (s=0.04)	*CN* (s=0.04)
D B S	0.97	3.2
D S SPLITD	1.00	4.7
D S SPLITB	0.92	4.8
B S SPLITD	0.83	5.3
B S SPLITB	0.87	4.8

- *Pairing:*

The ***RGA*** analysis indicates that the *D S B* is the best pairing for the *D B S* set of manipulated variables. In Figure 4.18, the ***RGA*** diagonal elements for this paired control structure are plotted. The ***RGA*** values at low frequencies are very large due to the transfer function singularity at steady state. However, ***RGA*** values at the most interesting frequencies (around 0.04) are good.

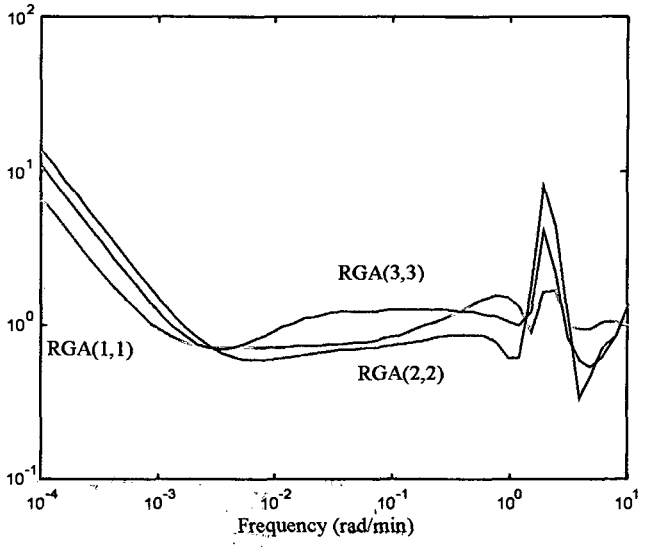

Figure 4.18: ***RGA*** diagonal elements of *D S B* control structure

The ***RGA*** plots are done using the reduced linear models and repeated with varying matrixes from the MATLAB μ-Analysis and Synthesis Toolbox (MATLAB, 1998). In both cases, very similar plots are obtained.

Optimal operation

At s=0.06, the singular value decomposition results show that the best structure is *D S B*, with *MRI*=0.46 and *CN*=3.2.

With "LV" inventory control, the change of the tuning of the inventory control has an effect on the composition control. For the non-optimal operation example and inventory control tuning of 0.53 and 0.60, the best structure is *D S SPLITD*. However, with inventory control tuning of 5.3 and 6.0, and with tighter tunings, the best structure is *D B S*. For the optimal operation, this influence of the tuning in the best structure is also found: with a tuning of 0.039 and 0.045, the best structure is *D S SPLITB* while it is *D B S* with a tuning of 0.39 and 0.45, and tighter tunings. For both examples, optimal and non-optimal operation, with loose inventory controls, *D S SPLITD* structure is preferred, and with tight inventory controls, *D B S* structure is preferred. The difference between the non-optimal and the optimal operations is that for some range of inventory controller tunings, the optimal operation already prefers the *D B S* and the non-optimal operation still prefers *D S SPLITD*. The preferred structure that would be obtained for perfect inventory control is *D B S*.

4.7.4.5 · Conclusions

Regarding at the whole set of singular value decomposition and ***RGA*** results for the optimal and the non-optimal operation examples, all four inventory control structures taken into account, it is worth noticing that:

- According to *MRI*, *CN*, and ***RGA*** frequency dependent analysis, the preferred DWC control structures depend on the operating conditions. For "DB" inventory control, the best control structure for the non-optimal operation is *L SPLITD S*, while the best control structure for the optimal operation is *L S V*. Of all the stabilised DWC, the best control structure for the non-optimal operation is "DV" inventory control and *B SPLITD S* composition control, while the best control structure for the optimal operation is "LV" inventory control and *D S B* composition control.
- For the non-optimal operation, split variables (*SPLITD* and *SPLITB*) appear in the set of preferred manipulated variables, while they do not appear for optimal operation.
- For all DWC inventory control structures, the best sets of manipulated variables for the non-optimal operation have better performance indexes than the best sets for the optimal operation.

- The *CN* for "DB" inventory control case are larger than *CN* for the other inventory control structures.

- The preferred control structures depend on the tuning of the inventory control loops for "LB", "DV", and "LV" inventory control structures.

4.8 Tuning

The tuning of the three composition control loops of the DWC is one of the most complex control problems.

Fixing some stability margins is the base of many tuning methods. The approach has been used for the tuning of the DWC composition control loops, considering separately the tuning of every loop. Specifically, the method consists in fixing the Phase Margin and Gain Margin (PM and GM) to obtain the tuning parameters. For every loop, four equations are used to solve four unknowns. The equations are the phase and magnitude values of the closed-loop transfer functions at the PM and GM frequencies, w_{GM} and w_{PM}. The unknowns are K_c, τ_c, w_{GM} and w_{PM} (see equation 4.22). However, with the reduced transfer function as linear model, multiplicity of solutions has been found, what makes the tuning determination very difficult.

To tune a PI controller, a very extended method is to find the ultimate gain and ultimate frequency and compute the controller parameters from them trough the Ziegler-Nichols equations. This method is also based on stability margins. The ultimate gain k_u is the value of controller gain at which the loop is at the limit of stability with a proportional feedback controller. The frequency where this occurs is the ultimate frequency w_u.

The tuning of the DWC separation example at non-optimal operation, with "DB" *L SPLITD S* control structure is considered. When looking for the ultimate values of the L-x_{AD} loop, it is seen that it is very difficult to make the loop unstable. Very large K_c are needed. This is because of the immediate response of the output to the input assumed by the model. However, in reality, a delay will exist when the loop is closed due to the time needed for the measurement. To take this delay into account, a delay of 0.5 min is added to each control loop. The Pade approximation of order 3 has been used to put the delay in transfer function form (MATLAB, 1998). The singular value decomposition and ***RGA*** analysis are not affected by the addition of this delay.

In Figure 4.19, the Bode plot of ***G(1,1)*** is shown for the considered case, without the added delay and with it. ***G(1,1)*** is the transfer function for the L-x_{AD} loop, which has been calculated through numerical linearisation and scaled. The phase of the transfer function without delay (red line) crosses the –180 deg at a higher frequency, indicating a more difficult unstabilisation (Skogestad et al., 1996).

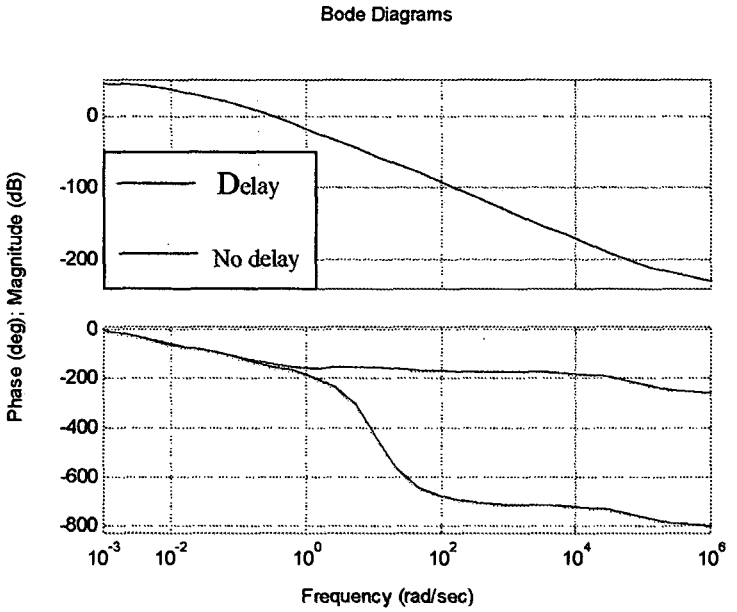

Figure 4.19: *G(1,1)* Bode plot

From the Bode plot shown in Figure 4.19, the values of ultimate gain k_u=6 and ultimate frequency w_u=0.73 rad for the *L*-x_{AD} loop are obtained. In the same way, for the *SPLITD*-x_{BS} loop, k_u=1.5 and w_u=1 rad are found, and for the *S*-x_{CB} loop, k_u=13 and w_u=0.9 rad are found. Comparing the Bode plots of *G(1,1)*, *G(2,2)*, and *G(3,3)*, it is seen that the phase crosses –180 deg for a much small frequency for *G*(2,2) and *G*(3,3) than for *G*(1,1). This is due to the slower response between the manipulated and the controlled variables for loops 2 and 3.

The Ziegler-Nichols gain and reset time constants for a PI controller can be calculated from equations 4.30, 4.31, and 4.32. For the studied example, K_c=2.7, τ_c=7.2 for the *L*-x_{AD} loop, K_c=0.68, τ_c=5.2 for the *SPLITD*-x_{BS} loop, and K_c=5.9, τ_c=5.8 for the *S*-x_{CB} loop.

$$K_c = k_u / 2.2 \qquad (4.30)$$

$$P_u(\text{min}) = 2\Pi / w_u(\text{rad/min}) \qquad (4.31)$$

$$\tau_c(\text{min}) = P_u(\text{min}) / 1.2 \qquad (4.32)$$

The Ziegler-Nichols rules are often not adequate for multivariable systems. For multivariable systems, it is needed a procedure that simultaneously tunes all controllers, taking into account the interaction that exists among the loops. The Biggest Log-modulus Tuning (BLT) is a way to accomplish this job. It provides settings that work reasonably well in many processes. These settings may not be optimum because they tend to be somewhat conservative. However, they guarantee stability and yield tunings that give a reasonable compromise between stability and performance in multivariable systems (Luyben, 1992).

The BLT method is based on the Ziegler-Nichols equations. The ultimate gain and ultimate frequency of each loop are calculated in the classical Single Input Single Output (SISO) way. A detuning factor F_{BLT} is assumed, which should be greater than 1. The larger the F_{BLT} value, the more stable the system will be, but more sluggish will be the system response. The gains of all feedback controllers (K_c) are calculated by dividing the Ziegler-Nichols gains by F_{BLT}. The feedback controller reset times (τ_c) are calculated by multiplying the Ziegler-Nichols reset times by F_{BLT}. To find the appropriate F_{BLT} value, L_{cm} has to be calculated.

$$L_{cm} = 20 * \log_{10} \left| \frac{W}{1+W} \right| \qquad (4.33)$$

where $W = -1 + det(\boldsymbol{I}+\boldsymbol{G}*\boldsymbol{K})$ and $\boldsymbol{K}$ is a diagonal matrix with the PI transfer functions of all loops as diagonal elements (see equation 4.22). The F_{BLT} factor is varied until the maximum value of L_{cm} is equal to $2N_{sys}$, being N_{sys} the order of the system.

For the DWC, N_{sys}=3. The BLT tuning method has been applied to the studied example and F_{BLT}=8 has been found. The resulting tuning is indicated in Table 4.7.

Table 4.7: BLT tuning for the non-optimal operation and "DB" *L* SPLITD *S* control structure

	K_c	τ_c (min)
Loop 1 (x_{AD} control)	0.340	57.3
Loop 2 (x_{BS} control)	0.085	41.8
Loop 3 (x_{CB} control)	0.740	46.5

A DWC simulation with tuning parameters in Table 4.7 is shown in Figures 4.20 and 4.21. A step change in the feed flowrate from 1 to1.1 kmol/min was applied as disturbance. In Figure 4.20, the output profiles are plotted. In Figure 4.21, the manipulated variables profiles are plotted. It can be seen that the BLT tuning time constant of the second loop (*SPLITD*- x_{BS}) is large.

But BLT tuning has some limitations. First of all, it makes the tuning more conservative than necessary applying the same F_{BLT} factor to all the loops, without analysing what loop causes the small stability margins. In addition, BLT tuning does not give appropriate tuning parameters for all DWC control structures. For instance, for the studied example at optimal operation conditions and "DB" *L S V* control structure, F_{BLT}=1 is found, for which K_c=6.31, τ_c=6.16 for the *L*-x_{AD} loop, K_c=17.7, τ_c=4.93 for the *S*-x_{BS} loop, and K_c=2.78, τ_c=2.92 for the *V*-x_{CB} loop. The non-scaled tuning parameters have very high gains (K_c =336 for the first loop), which are not correct.

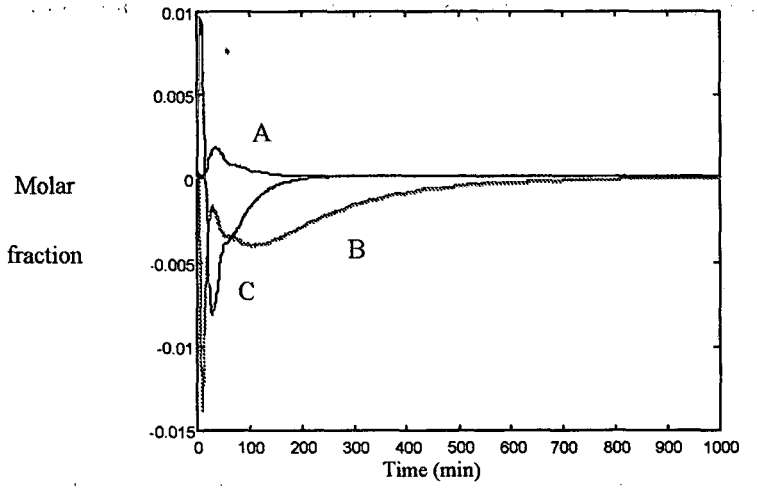

Figure 4.20: Output profiles for a disturbance in F

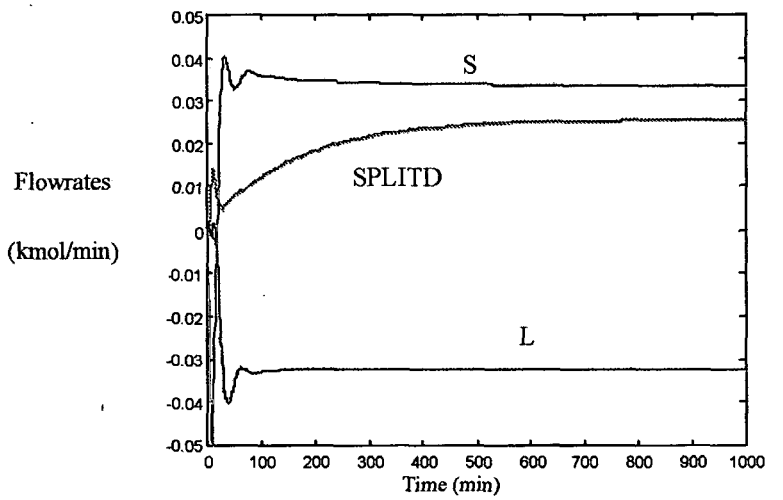

Figure 4.21: Input profiles for a disturbance in F

4.9 Simulations and comparisons

In section 4.7, the larger differences between the controllability indexes of the preferred control structures at optimal and non-optimal operations have been found for the "DB" stabilised DWC. The controllability of the non-optimal operation preferred control structure is better. Further comparisons between the preferred control structures of the "DB" optimal and non-optimal operations are performed in this section. The objective is to study the possible trade-off between operation optimisation and controllability. The preferred control structures of the "LV" optimal and non-optimal operations will be further studied too, because of the favourable controllability

indexes found, and because "LV" stabilising structure is recommended when reflux ratios are large.

Simulations are carried out to observe the behaviour of the controlled systems facing different disturbances. Step changes in disturbances have been considered. The analysis of this kind of signal is very useful because of its wide frequency content.

4.9.1 "DB" DWC: Comparison between *L SPLITD S* structure at non-optimal operation and *L S V* structure at optimal operation.

In this section, for the studied example at non-optimal operation, the preferred control structure, *L SPLITD S*, is considered. For the studied example at optimal operation, the preferred control structure, *L S V*, is considered (see Tables 4.2 and 4.3). Controllability and stability of both examples are analysed and compared.

CLDG and ***PRGA*** matrixes have been calculated and plotted for both examples. For the non-optimal operation example, they can be seen in Figure 4.22. From ***CLDG*** plots, it is seen that the disturbance more difficult to reject is q_F for output 1 (x_{AD}). Comparing ***CLDG*** and ***PRGA*** plots, it is seen that the setpoint tracking is easier than the disturbance rejection (remember that ***PRGA*** values at high frequencies are not relevant if only setpoint tracking at low frequencies is required). Therefore, if disturbance rejection is achieved, setpoint tracking will be achieved, too.

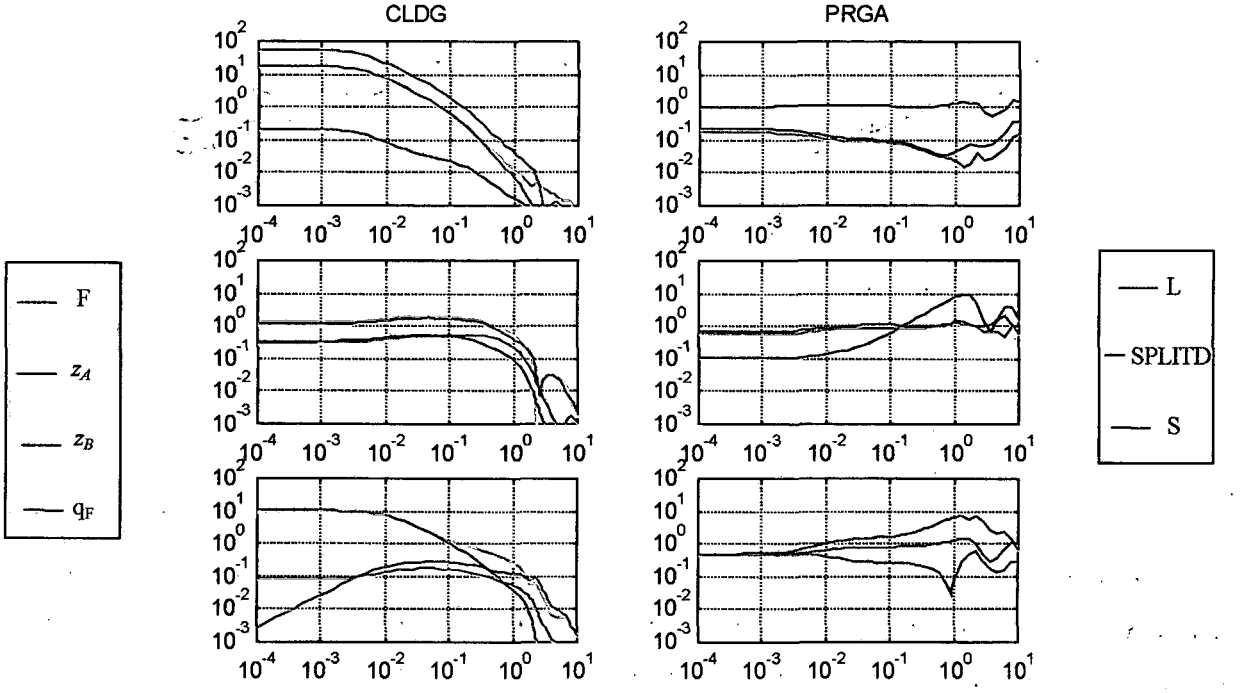

Figure 4.22: ***CLDG*** and ***PRGA*** for the non-optimal operation. First row plots are for output1, second row plots are for output 2, and third row plots are for output 3.

CLDG and *PRGA* for the optimal operation example are shown in Figure 4.23. From *CLDG* plots, it is seen that the disturbance more difficult to reject is F for output 3 (x_{CB}). From the *PRGA* plots, it is seen that the setpoint change more difficult to achieve is the setpoint change of output 3 (x_{CB}). Notice that the disturbance and the setpoint change that will impose more tight control tuning are not the same for the two examples. Notice also that in general, *CLDG* and *PRGA* values are larger for the optimal operation, which indicates a more difficult control. Specially, the *PRGA* values are much larger for the optimal operation than for the non-optimal operation.

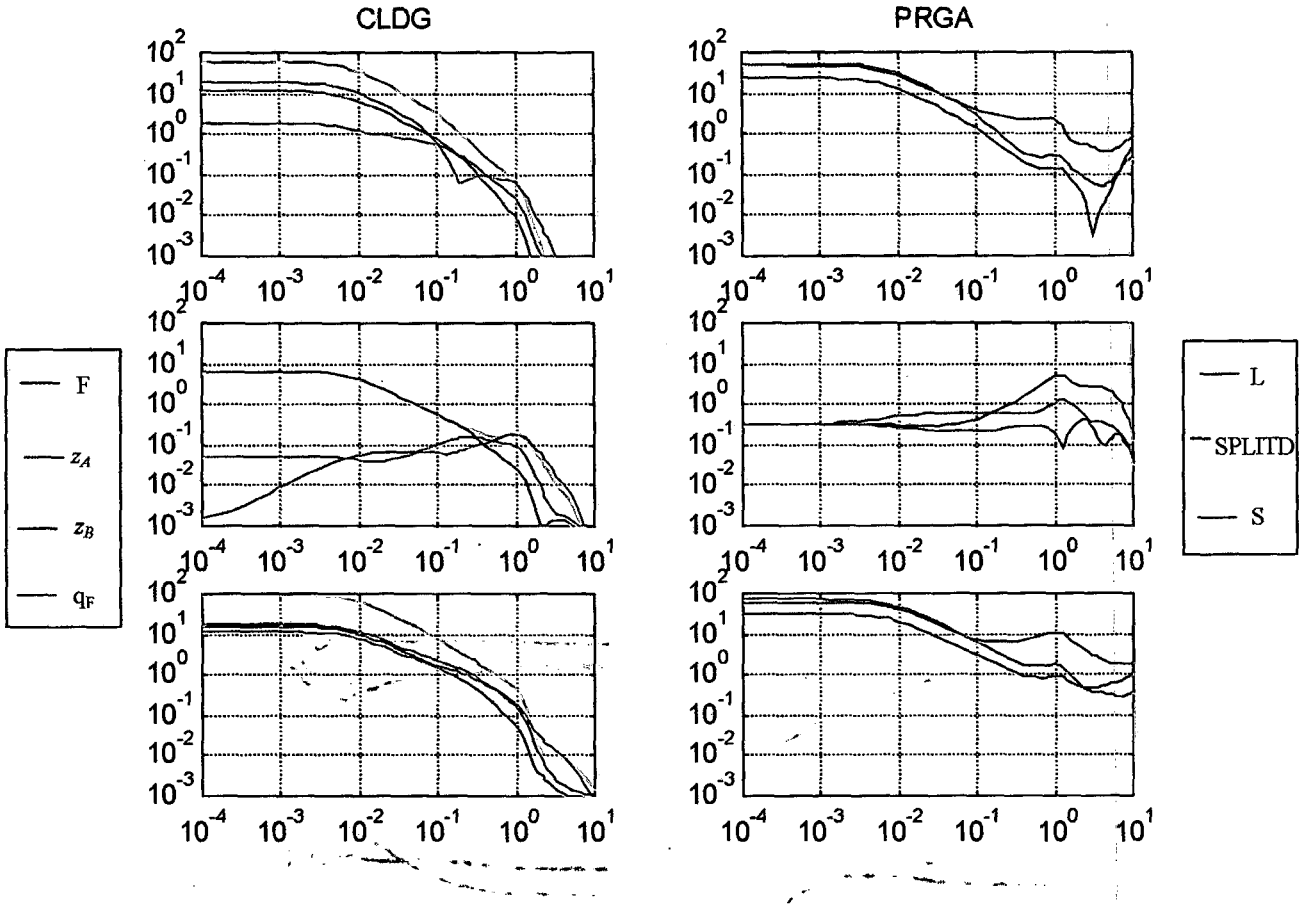

Figure 4.23: *CLDG* and *PRGA* for optimal operation. First row plots are for output1, second row plots are for output 2, and third row plots are for output 3.

To tune the two control systems in such a way that the control performances are similar is difficult because of the great quantity of performance parameters that can be regarded for MIMO systems. With comparison purposes, tunings which give similar output responses for the more demanding disturbances have been chosen. They are indicated in Table 4.8. In Figures 4.24 and 4.25, the behaviour of the two control systems is shown when a step change is applied to the feed vapour fraction (from q_F=1 to q_F=0.9). In Figures 4.26 and 4.27, the behaviour of the two control

systems is shown when a step change is applied to the feed flowrate (from F=1 kmol/min to F=1.1 kmol/min).

Table 4.8: tunings of the "DB" DWC preferred control structures

	Non-optimal column		Optimal column	
	K_c	τ_c (min)	K_c	τ_c (min)
Loop 1 (x_{AD} control)	0.37	66	0.38	75
Loop 2 (x_{BS} control)	0.45	16	-2.25	75
Loop 3 (x_{CB} control)	3.00	66	0.33	75

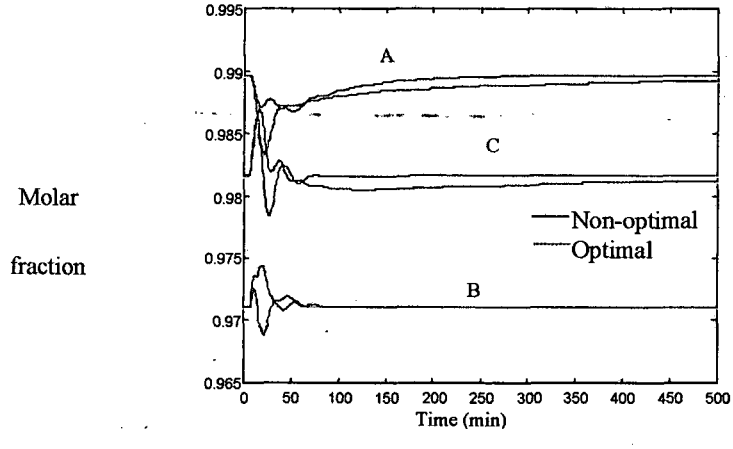

Figure 4.24: Output profiles for a disturbance in q_F

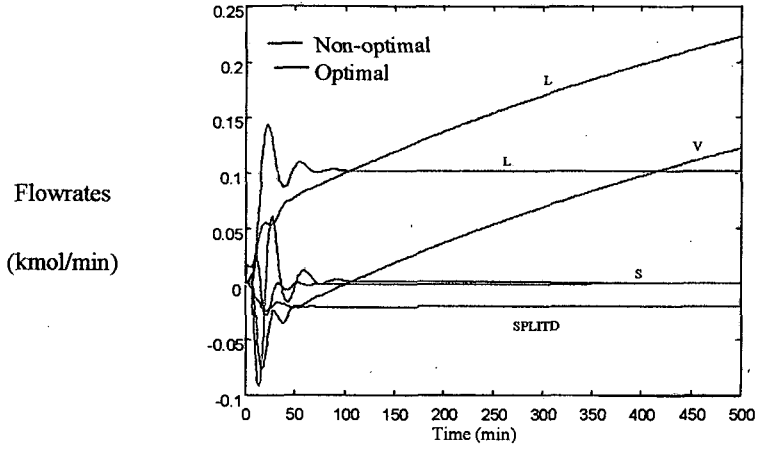

Figure 4.25: Input profiles for a disturbance in q_F

In Figures 4.24 and 4.25, it is seen that the convergence of loops 1 and 3 is very slow for the optimal operation example with L S V control structure. Large tuning changes are required to slightly improve the time responses. This occurs because L and V variables increase with similar rates and the reflux ratios increase very slowly. This effect can also be observed in Figures 4.26 and 4.27 for a disturbance in the feed flowrate.

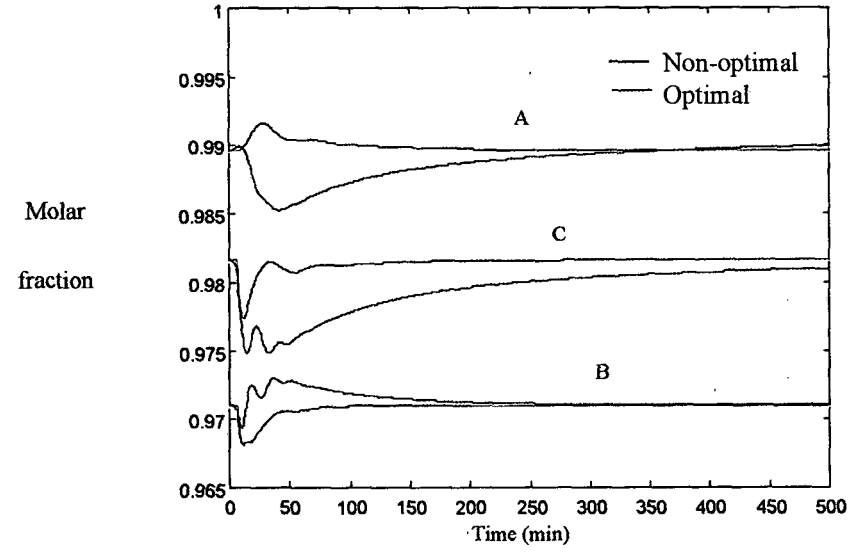

Figure 4.26: Output profiles for a disturbance in F

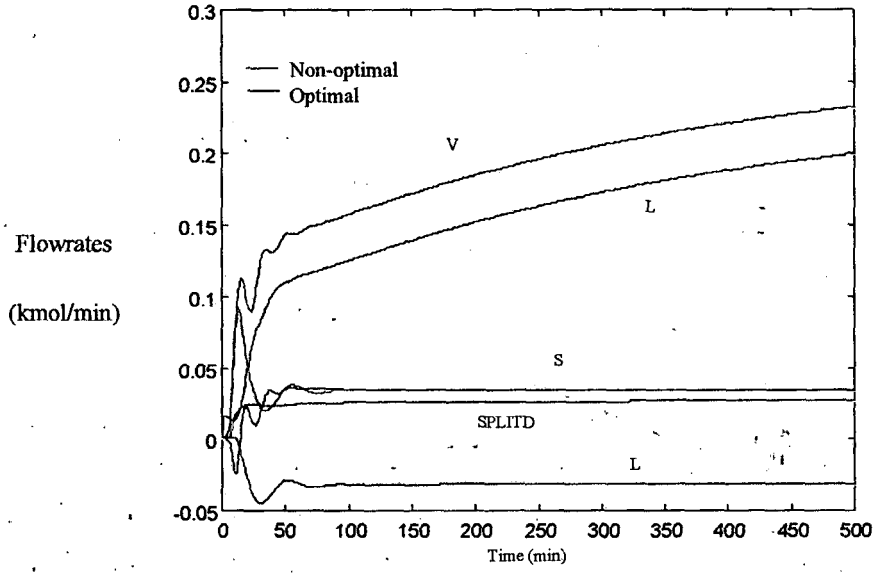

Figure 4.27: Input profiles for a disturbance in F

In Figure 4.28, the maximum and minimum S singular values are plot for the two examples. S is a good indicator of closed loop performance (Skogestad, 1996). Typical specifications in terms of S include large bandwidth frequency (frequency where max(σ(S(jw))) crosses 0,707 from below) and a peak of max(σ(S(jw)) smaller than 2. Larger peaks indicate poor performance as well as poor robustness. In Figure 4.28, a notable difference is seen between the bandwidth of the two systems, being larger that of the non-optimal operation case. Having the maximum and the minimum S singular values very different values, the L S V structure (optimal operation case) shows the high directionality already indicated by the simulations and the high CN. On the other hand, similar peaks are found for both examples, both of them larger than two.

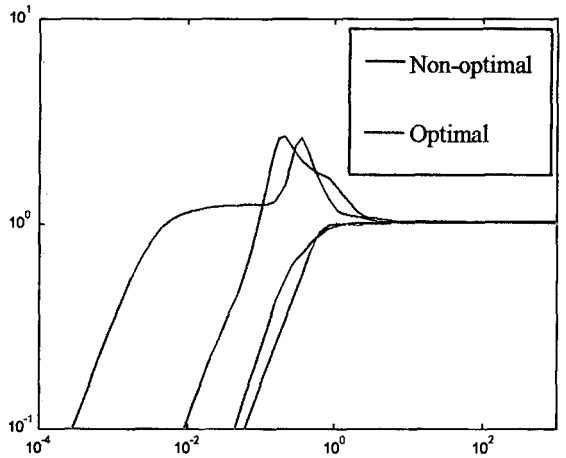

Figure 4.28: maximum and minimum S singular values

Having tuned the two examples to have similar performance, it will be interesting to study the stability of the two control systems. It is difficult to generalise the GM and PM to MIMO systems. However, the maximum peak criterion may be easily generalised replacing absolute values in SISO for maximum singular values in MIMO (Luyben, 1992). The criterion require that the maximum value of the maximum singular value of the complementary sensitivity function T ($T=G^*K^*(I+G^*K)^{-1}$) is smaller than 2 for robust stability.

$$\max(\bar{\sigma}(T(jw))) \leq 2 \quad (4.34)$$

The maximum peak criterion can be insufficient for MIMO systems for which advanced tools considering uncertainty descriptions (μ-analysis) are needed. However, to have a first idea of the stability robustness, in Figure 4.29, the maximum singular value of T is shown for the two examples. Both systems present a maximum value greater than two, indicating possible stability problems in front of uncertainties.

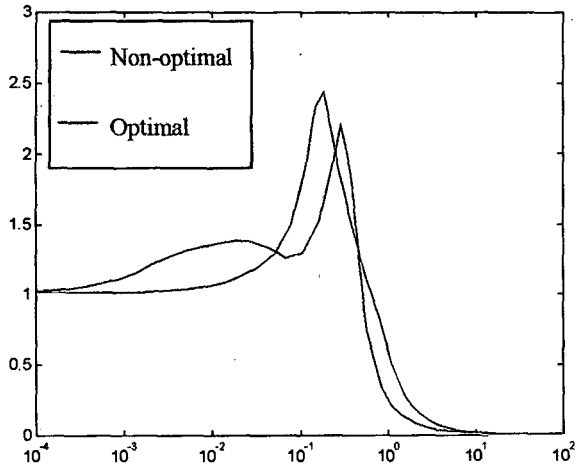

Figure 4.29: max(σ (***T***))

Another simple method to analyse stability is based on the plot of the maximum singular value of w_I*T_I (T_I=***KG(I+KG)***$^{-1}$). Robust stability is satisfied if at all frequencies equation 4.35 is fulfilled, where w_I is the uncertainty in input channels.

$$\bar{\sigma}(w_I * T_I(jw)) < 1 \quad (4.35)$$

This is a conservative condition of robust stability because it assumes full-block uncertainty, which is not reasonable for all plants (Luyben, 1992). Since no information about the uncertainty is available, the w_I proposed by Skogestad et al. (1996) and Morari et al. (1989) for a distillation column example is assumed. It corresponds to a 20 % gain error and a neglected time delay of 0.9 min. Its transfer function is shown in 4.36.

$$w_I(s) = 0.2\frac{5s+1}{0.5s+1} \quad (4.36)$$

In Figure 4.30, the maximum singular value of w_I*T_I is plotted for the two examples. Both structures would have problems with robust stability for full-block w_I uncertainty because they violate the robust stability condition.

Since all results in this section depend on the chosen tuning, a different tuning for the non-optimal example is chosen to see its influence on performance and stability. The new chosen tuning is shown in Table 4.9. Compared to the initial tuning (Table 4.8, two first columns), it is more conservative.

In Figure 4.31, the output profiles for a disturbance in the feed vapour fraction (from q_F=1 to q_F=0.9) are shown. In Figure 4.32, the input profiles for the same simulation are shown. It is seen that the new (less aggressive) tuning gives higher output overshoots and smoother input changes.

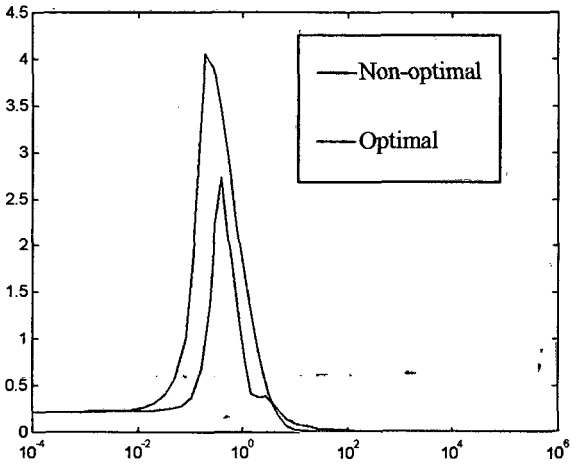

Figure 4.30: max(σ *(wi*T)*)

Table 4.9: New tuning for the example at non-optimal operation

	K_c	τ_c (min)
Loop 1 (x_{AD} control)	0.19	50
Loop 2 (x_{BS} control)	0.23	25
Loop 3 (x_{CB} control)	0.90	120

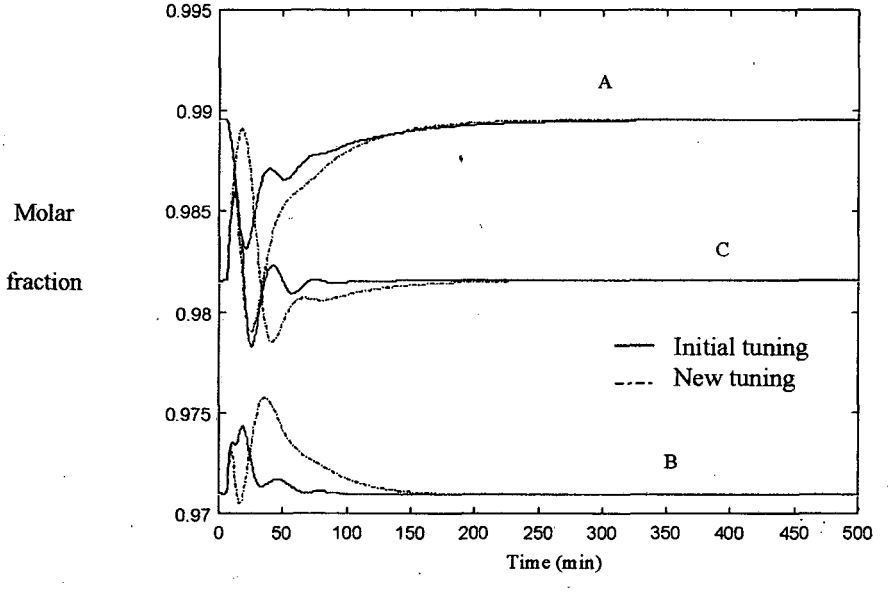

Figure 4.31: Output profiles for two different tunings

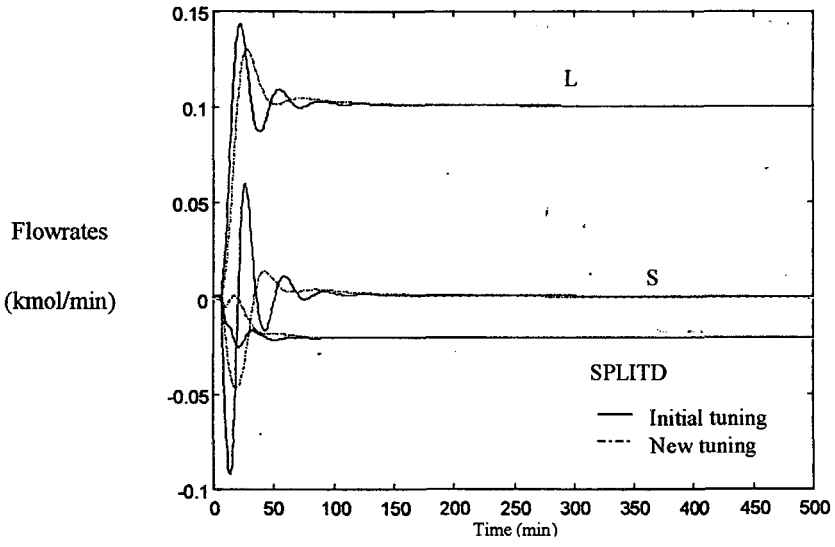

Figure 4.32: Input profiles for two different tunings

In Figure 4.33, the minimum ***S*** singular value for both tunings is plotted. With the new tuning, the bandwidth frequency has diminished. However, it continues to be notably higher than the one of the optimal column (compare Figures 4.33 and 4.28). The influence of the tuning on the bandwidth frequency is quite large, what indicates that a repeated frequency analysis at the known bandwidth frequency would be appropriate. In sections 4.11.2.1 and 4.11.2.2, and in chapter seven, this analysis will be performed.

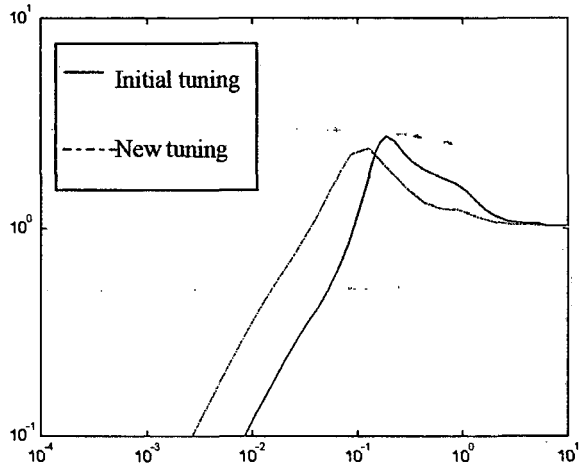

Figure 4.33: minimum ***S*** singular value

In Figure 4.34, the plot of the T maximum singular value can be seen for the two tunings. The peaks of the two curves are not very different. In any case, the peak of the new tuning is still larger than 2, indicating possible stability problems in front of uncertainties.

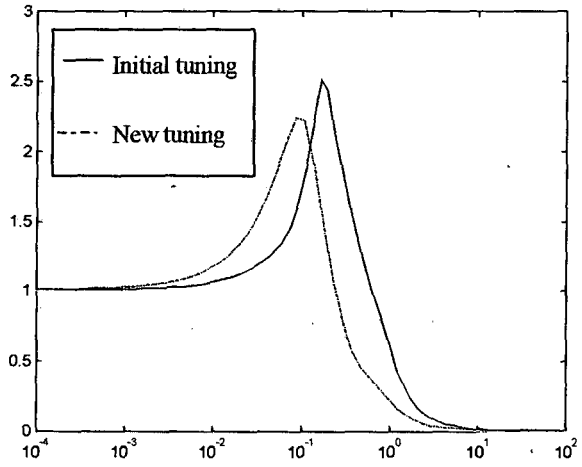

Figure 4.34: max(σ (T))

Finally, in Figure 4.35, the maximum singular value of $wi*T$ is plot for the two tunings. It can be seen that the peak is lower for the new tuning. However, it is still larger than 1, indicating possible problems with robust stability for full-block w_I uncertainty.

Analysing other tunings, it is seen that both control structures "DB" L S V and "DB" *L SPLITD S* have large stability margins for some tuning parameters. In base of the tunings given in Table 4.8, for "DB" *L S V* structure, making the tuning of loop 2 looser, max(σ($wi*T$)) is smaller than one. For "DB" *L SPLITD S* structure, making loop 3 looser, max(σ($wi*T$)) is smaller than one. In chapter five, examples of "DB" *L S V* control structure for which stability margins are sufficient for robust stability will be studied.

Having introduced a new tuning, it has been seen that the tuning influence on the control system performance and on the system stability is large, what makes the comparison task still more complex. In coming chapters, especially in chapter seven, this fact is taken into account in controllability and stability analysis.

Concluding this section, from the comparison between the studied example at optimal and non-optimal operating conditions, it can be said that controllability would be better operating at non-optimal conditions. MRI, CN, RGA, CLDG, PRGA, and simulations indicate this. Therefore, a trade-off is found between controllability and energy optimality for the "DB" inventory controlled DWC. On the other hand, stability robustness at both operating conditions could be problematic. A more detailed study including μ-analysis (Morari et al., 1989) would be required.

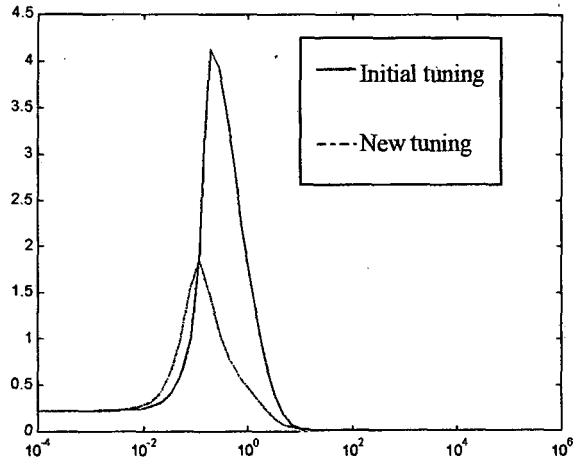

Figure 4.35: max(σ(*wi***T*))

4.9.2 "LV" DWC: *D S B* structure for non-optimal operation and optimal operation.

For the studied separation, with "LV" stabilisation, the preferred control structures at optimal and non-optimal operating conditions are the same. This structure is *D S B*. Since in this section, processes with the same control structure will be compared, to have a base for comparison, the same tunings are assumed. They are indicated in Table 4.10.

Table 4.10: Tuning for both examples, operation at optimal and non-optimal conditions

	K_c	τ_c(min)
Loop 1 (x_{AD} control)	-1.2	80
Loop 2 (x_{AD} control)	-1.2	80
Loop 3 (x_{AD} control)	-1.2	80

The responses of the controlled systems to a change in *F* from 1 kmol/min to 1.1 kmol/min are shown in Figures 4.36 and 4.37. A step change was applied to the disturbance variable during 10 minutes. In Figure 4.36 the output profiles have been plotted. In Figure 4.37, the input profiles have been plotted. It can be seen that performances of the two control systems are similar.

In Figure 4.38, the maximum and minimum ***S*** singular values can be seen for the two operating conditions. The plots of the maximum singular value of ***T*** can be seen in Figure 4.39. Finally, in Figure 4.40, the plots of the *wi***T* maxim singular value are shown. Regarding ***S*** plot, the bandwidth of the two systems is seen to be very similar and none of the systems has a peak larger than two, indicating good performance and robustness. From the plot of max(σ (***T***)), no

stability problems are indicated, and neither from the plot of max(σ(*wi*T*)). Even this conservative stability criterion indicates that both control systems would have robust stability in front of uncertainties.

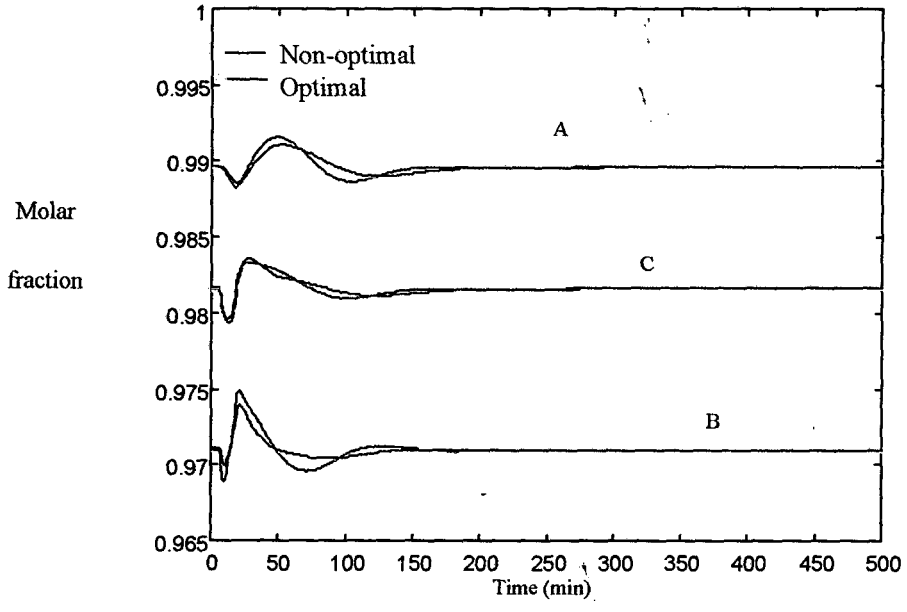

Figure 4.36: Output profiles for a disturbance in *F*

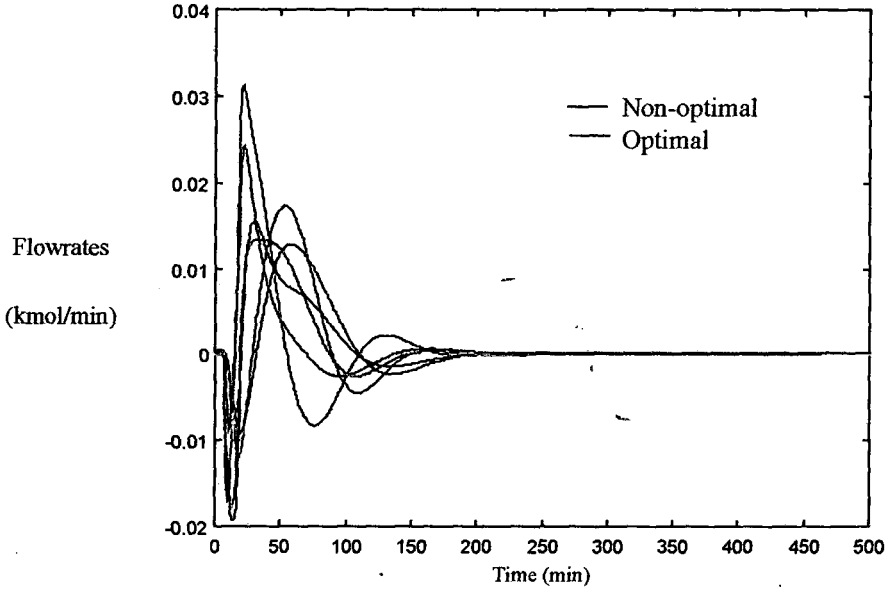

Figure 4.37 : Input profiles for a disturbance in *F*

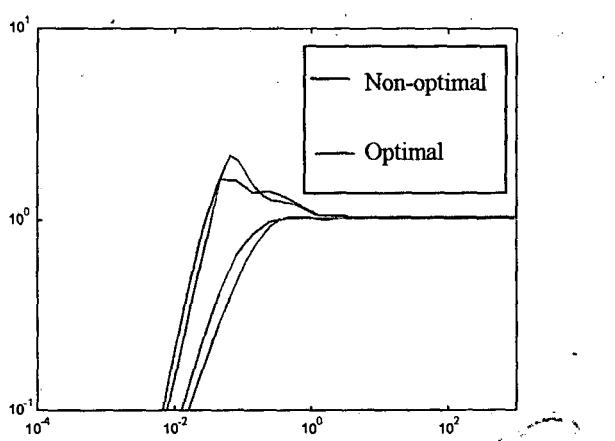

Figure 4.38: maximum and minimum ***S*** singular values

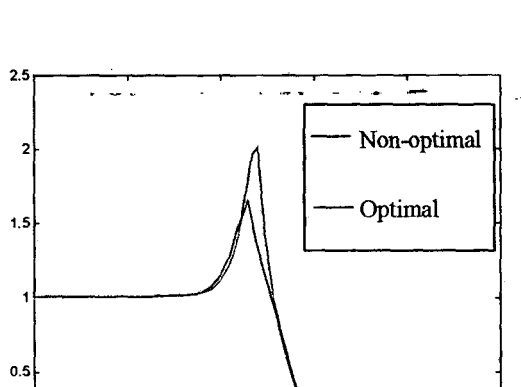

Figure 4.39: max(σ (***T***))

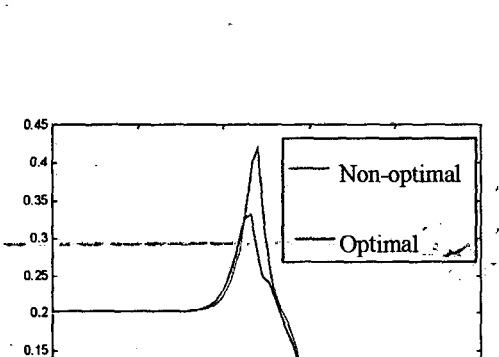

Figure 4.40: max(σ(*wi*****T***))

Comparing the stability analysis in sections 4.9.1 and 4.9.2, it is seen that the stability margins of the "LV" best control structure are larger than the stability margins of the "DB" best control structures (compare Figures 4.30 and 4.40).

With "LV" inventory control and *D S B* composition control structure, the DWC has shown good controllability indexes and large stability margins at optimal and non-optimal operating conditions. Controllability and stability are found to be similar at optimal and non-optimal operating conditions. Only a better *MRI* for the non-optimal operation case has been found. Therefore, it does not seem that a trade-off is possible between controllability and operation optimality with "LV" inventory control.

4.10 Logarithm of compositions

In section 4.3.2.3, it was seen that the system under study is very non-linear. This is the case of most distillation systems. However, it turns out that the process response is much less dependent on the operating point if instead of considering the compositions, the logarithmic compositions are considered. Normally, the logarithmic composition is defined as the logarithm of the ratio between the compositions of the key components,

$$y=\ln(x_L/x_H) \qquad (4.37)$$

where x_L and x_H are the compositions of the high and heavy key components.

In this section, the control of the DWC product compositions through their logarithms is considered through an example. The separation described in 4.3.1.2 (non-optimal operating conditions) with "DB" inventory control is chosen. The product composition logarithms have been considered the output variables. The linearisation has been done as explained in section 4.3.2.3 and the system scaled as explained in section 4.3.2.4.

Singular value decomposition at s=0.04 has been given special importance because the larger ***A*** eigenvalue is -0.004. The preferred composition control structures and their *MRI* and *CN* at s=0.04 are indicated in Table 4.11. Table 4.2 corresponds to the same case study considered in this section but with the product compositions as output variables instead of the logarithm of the product compositions as output variables. Comparing Tables 4.2 and 4.11, it is seen that the preferred control structures are the same. Also, it is seen that the *MRI* are much larger and the *CN* smaller for the case with logarithms of product compositions as output variables. Therefore, according to these indexes, the control of the logarithms of the product compositions improves the controllability.

The ***RGA*** analysis indicates that a crossed pairing is preferred (*SPLITD* controlling the B composition and *S* controlling the C composition). In Figure 4.41, the ***RGA*** diagonal elements for the *L SPLITD S* paired control structure are plotted. As can be seen comparing Figures 4.11

and 4.41, ***RGA*** does not change because of the consideration of the logarithms as output variables.

Table 4.11: Controllability indexes at s=0.04 for "DB" inventory control

Control structure	*MRI*	*CN*
LVS	37.7	70
LSSPLITD	107	16
LSSPLITB	105	17
VSSPLITD	107	18
VSSPLITB	106	19

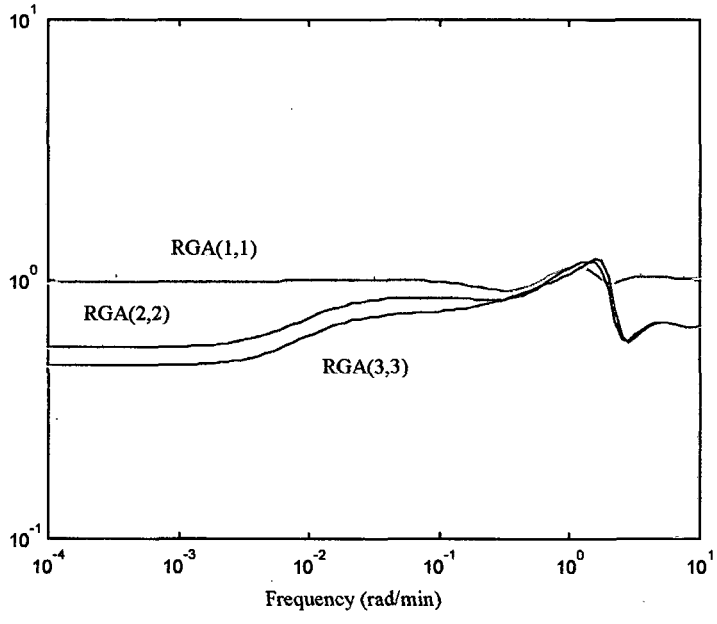

Figure 4.41: ***RGA*** diagonal elements for *L SPLITD S* control structure

To illustrate the system behaviour, the system response to a disturbance in q_F is simulated. In Figures 4.42 and 4.43, the product compositions and input profiles are plotted. The corresponding tuning parameters can be seen in Table 4.12. In Figures 4.24 and 4.25, control responses to the same disturbance and identical conditions were shown. In that case, however, the product compositions were directly controlled instead of controlling the logarithms of the product compositions. Comparing Figures 4.24 and 4.25 with Figures 4.42 and 4.43, it can be seen that the input variations are more sluggish and the time responses shorter in Figures 4.42 and 4.43. Therefore, in accordance with the results given by the controllability indexes,

simulation results indicate that the control of the logarithms of the product compositions improves the controllability.

Table 4.12: Tuning for the control of the logarithms of the compositions

	K_c	τ_c (min)
Loop 1 ($\ln(x_{AD})$ control)	9.80	33
Loop 2 ($\ln(x_{AD})$ control)	0.62	6
Loop 3 ($\ln(x_{AD})$ control)	2.49	83

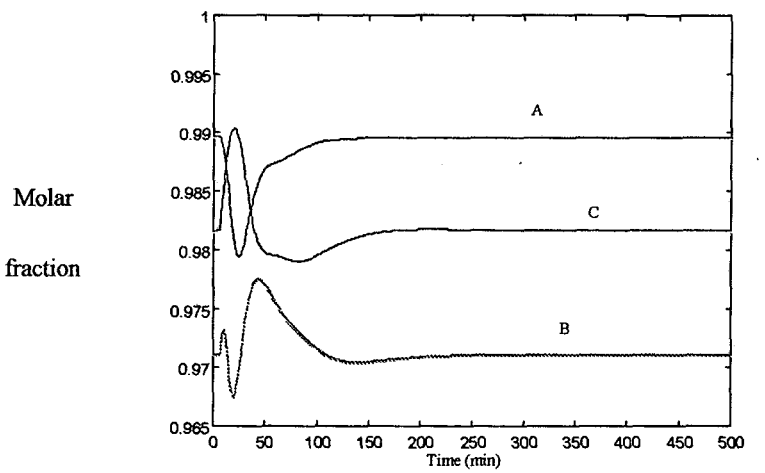

Figure 4.42: Product composition profiles for a disturbance in q_F

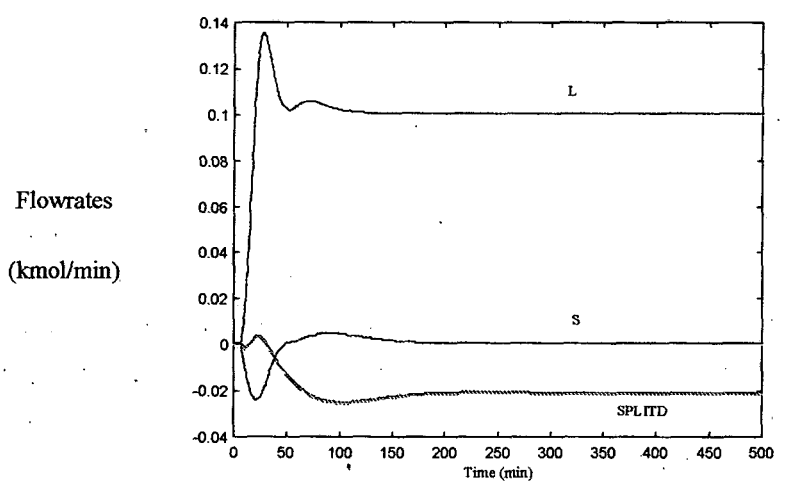

Figure 4.43: Input profiles for a disturbance in q_F

4.11 Generalisation

The aim of this section is to explore, through the consideration of different examples, the generality of the results found in sections 4.7 and 4.9. Different mixtures and operating conditions are studied.

The considered DWC design in this section has *NT*=46, *NP*=13, *NM*=33, *NS*=17, *NCB*=8, *NCD*=26 and *NF*=7. In all cases, products are liquid saturated flows, feeds are liquid saturated equimolar flows, and separation into 0.99 molar pure products is required.

4.11.1 DWC controllability for the separation of three different mixtures

The separation of three different mixtures is studied in this section. Their sets of relative volatilities and *ESI* are:

- α=(4.65 : 2.15 : 1) *ESI*=1
- α=(4.56 : 1.85 : 1) *ESI*=1.36
- α=(4.65 : 2.45 : 1) *ESI*=0.77

Optimal operation is chosen in the three cases. The considered DWC design is the optimal design for the separation of the mixture with *ESI*=1, according to the design methodology described in 2.6.2.

In Tables 4.13, 4.14, and 4.15, the best control structures and their controllability indexes for the different stabilised columns and the different mixtures are indicated. *MRI* and *CN* values correspond to a frequency of 0.04. In some cases, the order of preference of control structures according to the *CN* is not the same that the order according to the *MRI*. For this reason, another index is used to classify the preferred structures. It is the Intersivity Index (*II*=*MRI*/*CN*). Large *II* are preferred.

Table 4.13: Preferred structures for the mixture with ESI=1

	"DB"	"LB"	"DV"	"LV"
First preferred structure	*L V S* *MRI*=0.25 *CN*=91	*V D S* *MRI*=0.29 *CN*=12	*L B S* *MRI*=0.28 *CN*=11	*D B S* *MRI*=0.34 *CN*=4.6
Second preferred structure	*L V PLITB* *MRI*=0.08 *CN*=272	*V S SPLITB* *MRI*=0.10 *CN*=27	*L B SPLITD* *MRI*=0.08 *CN*=30	*B S SPLITB* *MRI*=0.1 *CN*=12

Table 4.14: Preferred structures for the mixture with *ESI*=1.36

s=0.04	"DB"	"LB"	"DV"	"LV"
First preferred structure	*L V S* *MRI*=0.16 *CN*=264	*V D S* *MRI*=0.14 *CN*=34	*L B S* *MRI*=0.14 *CN*=35	*D B S* *MRI*=0.12 *CN*=14
Second preferred structure	*S SPLITD PLITB* *MRI*=0.009 *CN*=139	*V D SPLITD* *MRI*=0.04 *CN*=116	*L B SPLITD* *MRI*=0.04 *CN*=117	*D B SPLITD* *MRI*=0.04 *CN*=42

Table 4.15: Preferred structures for the mixture with *ESI*=0.77

s=0.04	"DB"	"LB"	"DV"	"LV"
First preferred structure	*L V S* *MRI*=0.20 *CN*=184	*V D S* *MRI*=0.18 *CN*=28	*L B S* *MRI*=0.19 *CN*=18	*D B S* *MRI*=0.17 *CN*=10
Second preferred structure	*S SPLITD PLITB* *MRI*=0.026 *CN*=77	*D S SPLITD* *MRI*=0.07 *CN*=38	*L B SPLITD* *MRI*=0.10 *CN*=36	*D B SPLITD* *MRI*=0.09 *CN*=18

Regarding at Tables 4.13, 4.14, and 4.15, the following can be observed:

- The preferred control structure do not depend on the separated mixture. This is true for the four inventory control structures. For the separation example at optimal operating conditions studied in section 4.7.4, the same preferred control structures were found for all four inventory control structures. Therefore, some generality can be presumed about preferred control structures.

- In none of the cases, the preferred control structures have *SPLITD* or *SPLITB* variables chosen for composition control. This was also true for the separation example at optimal operating conditions studied in section 4.7.4. Therefore, some generality can be presumed, too.

- The *MRI* and *CN* controllability indexes indicate that the preferred structure with "DB" inventory control is the worst of all the preferred structures for the different inventory controls, and the preferred structure with "LV" inventory control is the best of all the

preferred structures for the different inventory controls. This is true for all three studied mixtures, what indicates some generality. Specifically, it is the *CN* index which is very large for control structures with "DB" inventory controls, and small for control structures with "LV" inventory controls.

- The separation of the mixture with *ESI*=1, which is the only with optimal design, has the best controllability indexes for all the inventory controls. It can be wondered if optimal design leads to better controllable columns. In chapter seven, the influence of the DWC design on the controllability will be studied.
- Comparing the *MRI* and *CN* values in this section with values obtained for the separation example at optimal operating conditions studied in section 4.7.4, it is seen that in general, controllability indexes were much better in that case. This is not rare since different product purities were specified.

4.11.1.1 Further analysis of the "LV" D *S* B control structure

For the three separation examples of the three different considered mixtures, with "LV", the same control structure is preferred, which is *D S B*. Of all the considered control structures, "LV" *D S B* has given the best *II*. In this section, ***RGA***, ***PRGA***, and ***CLDG*** of this structure for the three separation examples are analysed.

For the separation of the mixture with *ESI*=1, the ***RGA*** diagonal elements are shown in Figure 4.44. For the separation of the mixture with *ESI*=1.36, they are shown in Figure 4.45. For the separation of the mixture with *ESI*=0.77, they are shown in Figure 4.46.

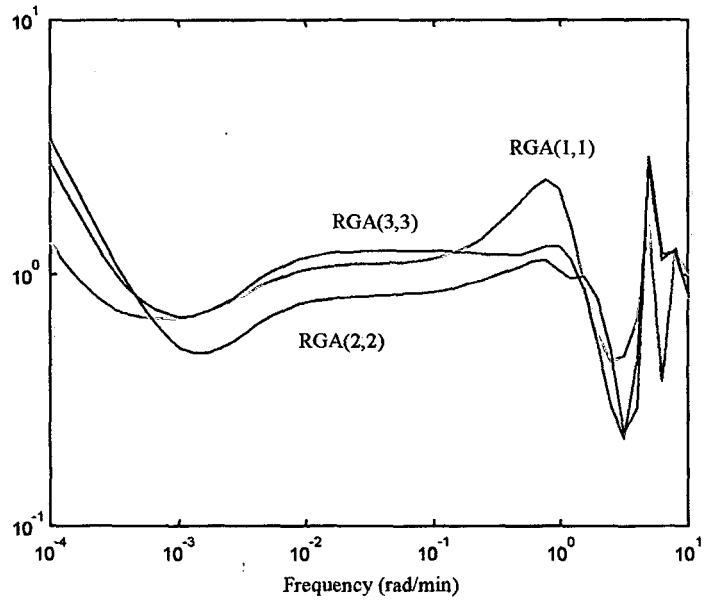

Figure 4.44: ***RGA*** diagonal elements for separation of the mixture with *ESI*=1

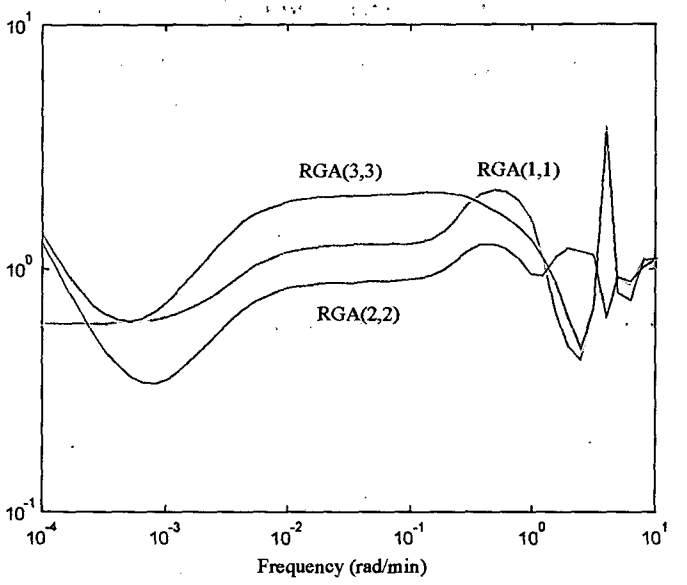

Figure 4.45: ***RGA*** diagonal elements for the separation of the mixture with *ESI*=1.36

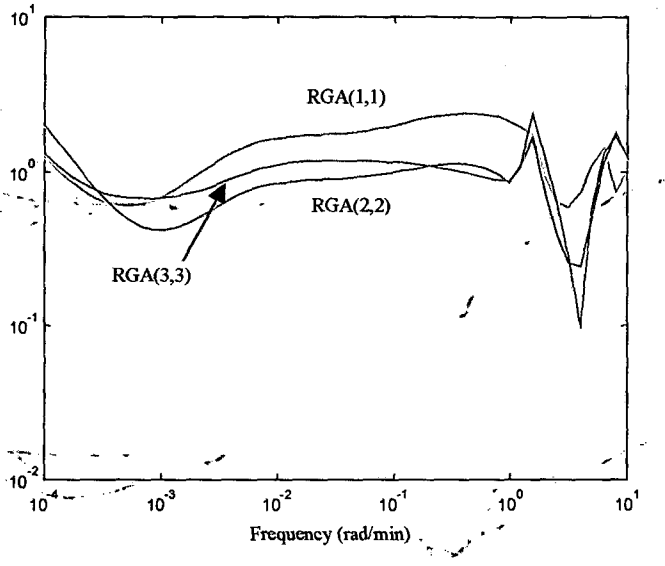

Figure 4.46: ***RGA*** diagonal elements for the separation of the mixture with *ESI*=0.77

The entire ***RGA*** matrix at s=0.04 for the separation of the mixture with *ESI*=1 is:

$$\begin{matrix} & D & S & B \end{matrix}$$

$$\boldsymbol{RGA}(0.04) = \begin{pmatrix} 1.08 & 0.14 & 0.21 \\ 0.21 & 0.81 & 0.02 \\ 0.28 & 0.06 & 1.21 \end{pmatrix} \begin{matrix} x_{AD} \\ x_{BS} \\ x_{CB} \end{matrix} \qquad (4.38)$$

The entire ***RGA*** matrix at s=0.04 for the separation of the mixture with *ESI*=1.36 is:

$$\boldsymbol{RGA}(0.04) = \begin{matrix} D & S & B \\ \end{matrix} \begin{pmatrix} 1.23 & 0.20 & 0.42 \\ 0.68 & 0.86 & 0.54 \\ 0.90 & 0.06 & 1.95 \end{pmatrix} \begin{matrix} x_{AD} \\ x_{BS} \\ x_{CB} \end{matrix} \qquad (4.39)$$

The entire ***RGA*** matrix at s=0.04 for the separation of the mixture with *ESI*=0.77 is:

$$\boldsymbol{RGA}(0.04) = \begin{matrix} D & S & B \\ \end{matrix} \begin{pmatrix} 1.74 & 0.11 & 0.68 \\ 0.47 & 0.89 & 0.54 \\ 0.32 & 0.16 & 1.15 \end{pmatrix} \begin{matrix} x_{AD} \\ x_{BS} \\ x_{CB} \end{matrix} \qquad (4.40)$$

From the ***RGA*** plots and numeric values, it is seen that the three systems have quite well behaved ***RGA***, indicating good controllability. However, in terms of ***RGA***, the separation of the mixture with *ESI*=1 has the best controllability. In this case, the ***RGA*** matrix is close to unity around the 0.04 frequency, which means that interaction between control loops is weak.

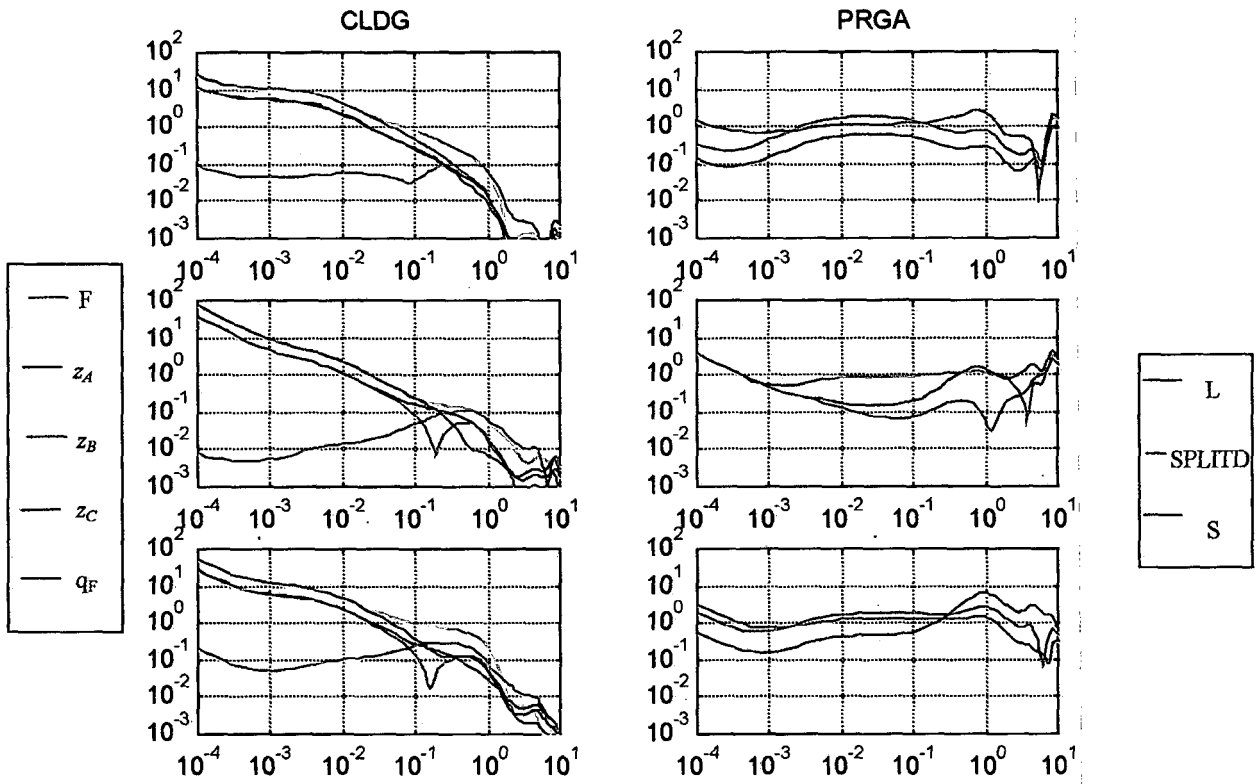

Figure 4.47: ***CLDG*** and ***PRGA*** for the separation of the mixture with ESI=1. First file plots are for output1, second file plots are for output 2, and third file plots are for output 3.

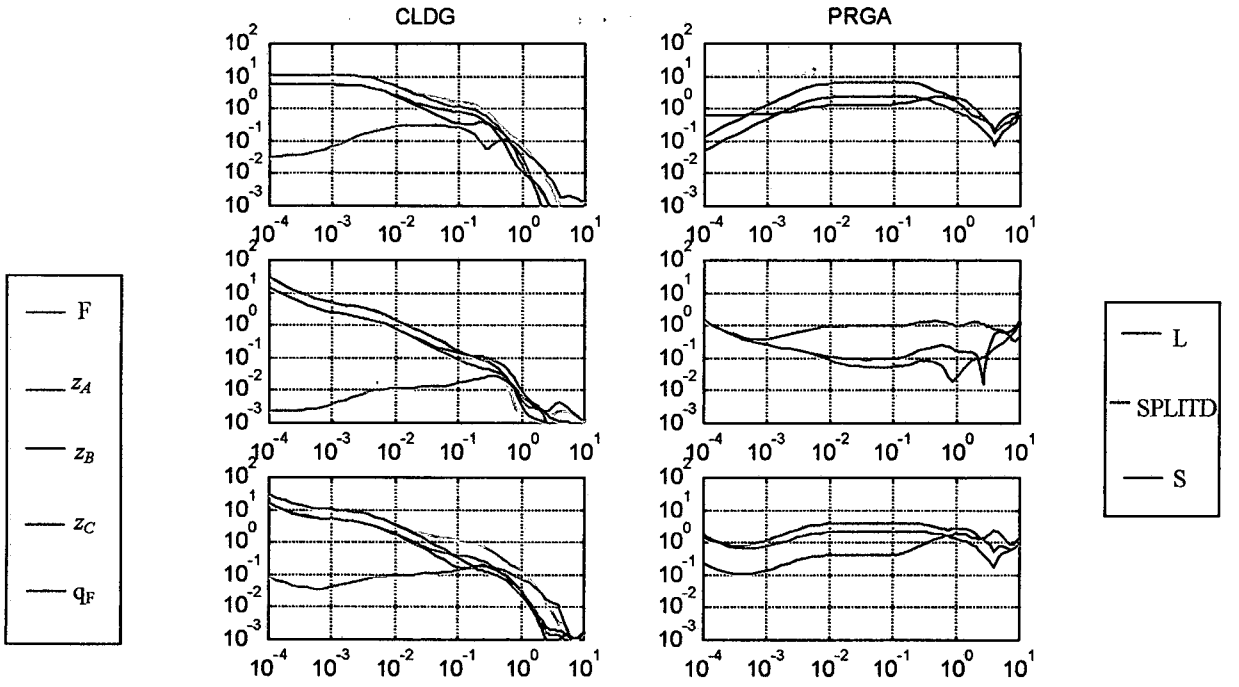

Figure 4.48: ***CLDG*** and ***PRGA*** for the separation of the mixture with ESI=1.36. First file plots are for output1, second file plots are for output 2, and third file plots are for output 3

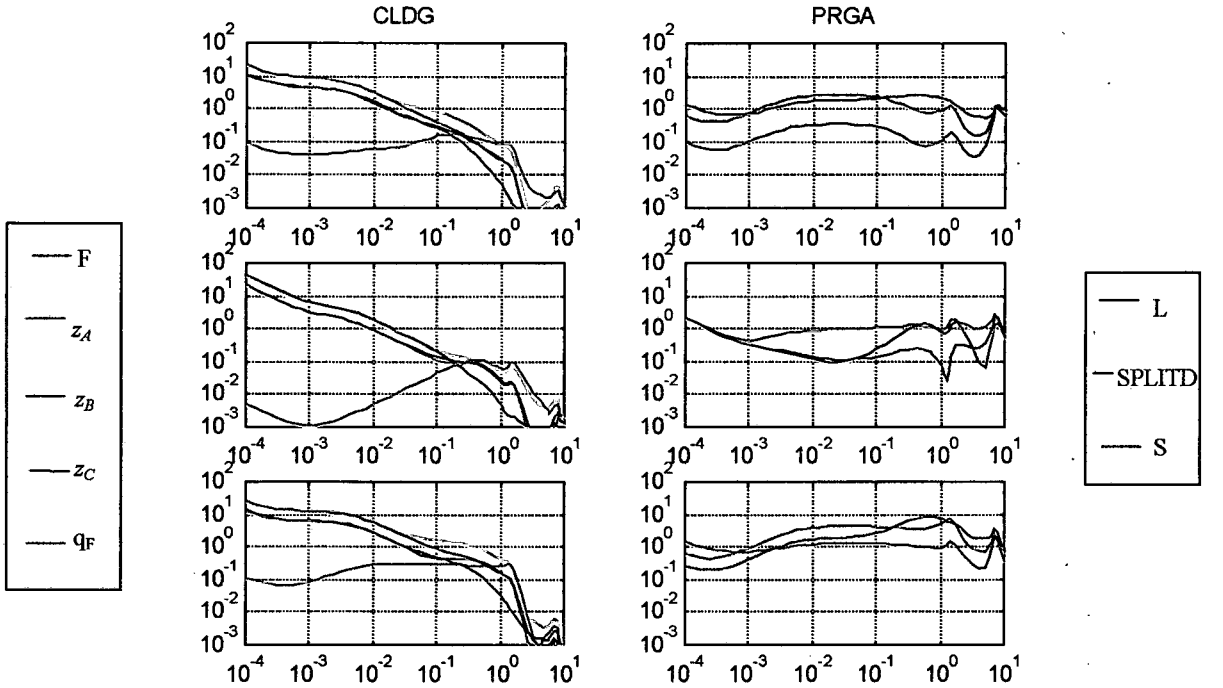

Figure 4.49: ***CLDG*** and ***PRGA*** for the separation of the mixture with ESI=0.77. First file plots are for output1, second file plots are for output 2, and third file plots are for output 3

Figure 4.47 shows the ***CLDG*** and ***PRGA*** for the separation of the mixture with *ESI*=1. Figure 4.48 shows the ***CLDG*** and ***PRGA*** for the separation of the mixture with *ESI*=1.36. And Figure 4.49 shows the ***CLDG*** and ***PRGA*** for the separation of the mixture with *ESI*=0.77. In all cases, *F* disturbance is found to be the most difficult to reject for the control of the three outputs. Also for the three examples, a disturbance in z_B for the control of output 2 appears very difficult to reject. The higher ***CLDG*** value is found for the mixture with *ESI*=1. On the other hand, setpoint changes appear more difficult for the separation of the mixture with *ESI*=1.36 (outputs 1 and 3), and for the separation of the mixture with *ESI*=0.77 (output-3). However, if setpoint tracking is only required at low frequencies, disturbance rejection is more difficult than setpoint tracking and therefore, if disturbance rejection is achieved, setpoint tracking will also be achieved.

4.11.2 Controllability at different operating conditions

In this section, the separation of the mixture with α=(4.65 : 2.15 : 1) is studied to compare the controllability of the DWC at different operating conditions. Three operating conditions have been studied. Optimal operation has been compared with two non-optimal operations, indicated as operation 1 and operation 2. Optimal operation has *SPLITD*=0.634 and *SPLITB*=0.500. Operation 1 was found fixing *SPLITD* at 0.614 and *SPLITB* at 0.500. Boilup increased a 3%. Operation 2 was found fixing *SPLITD* at 0.654 and *SPLITB* at 0.500. Boilup increased a 10%.

In Tables 4.16, 4.17, and 4.18, the preferred control structures for the different stabilised columns at the different operations are shown. When controllability with *SPLID* and *SPLITB* are similar, *SPLITD* has been chosen.

Table 4.16: Preferred structures at optimal operation (analysis at *s*=0.04 rad/min)

"DB"	"LB"	"DV"	"LV"
L V S	*V D S*	*L B S*	*D B S*
MRI=0.25	*MRI*=0.29	*MRI*=0.28	*MRI*=0.34
CN=91	*CN*=12	*CN*=11	*CN*=4.6

Table 4.17: Preferred structures at operation 1 (analysis at s=0.04 rad/min)

"DB"	"LB"	"DV"	"LV"
L S SPLITD	*D S SPLITD*	*B S SPLITD*	*B S SPLITB*
MRI=0.70	*MRI*=0.69	*MRI*=0.67	*MRI*=0.61
CN=23.18	*CN*=3.82	*CN*=3.86	*CN*=2.11

Table 4.18: Preferred structures at operation 2 (analysis at s=0.04 rad/min)

"DB"	"LB"	"DV"	"LV"
L S SPLITD	*D S SPLITD*	*B S SPLITD*	*D S SPLITB*
MRI=1.07	*MRI*=0.91	*MRI*=1.03	*MRI*=0.71
CN=16.09	*CN*=2.95	*CN*=2.61	*CN*=2.04

Comparing the results of Tables 4.16, 4.17, and 4.18, the following can be noticed:

- At optimal operation, the preferred sets of manipulated variables do not include the split variables. On the contrary, at the non-optimal operations, the preferred sets of manipulated variables include the split variables.
- For all inventory controls, non-optimal operation preferred control structures have better controllability indexes.

These conclusions coincide with the conclusions in section 4.7.4.5 for a different separation problem. This indicates that some generality of the results can be presumed.

4.11.2.1 "DB" inventory control

RGA analysis indicates *L SPLITD S* as the best paired structure for the non-optimal operations and *L S V* as the best paired structure for the optimal operation. PI controllers with K_c=1 and τ_c=80 are implemented to each control loop and the bandwidths are searched. *MRI* and *CN* at the bandwidth indicate the same preferred structures indicated at frequency 0.04 rad/min. According to the results, controllability of the non-optimal operations is better. Therefore, for "DB" inventory control, as found in section 4.9.1, a trade-off between controllability and energy optimality is possible.

Simulations showing the control performance of "DB" *L S V* structure at optimal operating conditions will be shown in section 5.9.1.

4.11.2.2 "LV" inventory control

With ***RGA*** analysis, the best paired structures are determined. PI controllers with K_c=1 and τ_c=80 are implemented to each control loop and the bandwidths are searched. At the bandwidth frequency, the preferred structure indicated by *II* for operation 1 is *D B S* instead of *B S SPLITB*, and the preferred structure indicated by *II* for operation 2 is *D S SPLITD* instead of *D S SPLITB*. At different frequencies, the controllability indexes indicate different preferred structures because their values for different control structures are similar. For optimal operation, the best structure is always *D S B*. A stability analysis through w_I*T_I maximum singular value indicates

robust stability for the three operations with their preferred structures. As was seen in 4.9.2, "LV" inventory control gives robust stability.

4.12 *L/D* and *V/B* as manipulated variables

Up to this point, the *L/D* and *V/B* ratios have not been considered as manipulated variables. However, some authors have stated their importance. *L/D V/B* structure for the control of distillate and bottoms products compositions in simple columns has been found to be the best one in some cases (Skogestad et al. 1990 b).

G(s) changes depending on the set of DOF chosen. For instance, the same ***G(s)*** is not obtained if the set of DOF is considered to be *L V S SPLITD PLITB* or if the set of DOF is considered to be *L/D V S SPLITD SPLITB*. Specifically, for a DWC with "DB" inventory control, there are four possible sets of DOF: *L V S SPLITD PLITB*, *L/D V S SPLITD SPLITB*, *L V/B S SPLITD SPLITB* and *L/D V/B S SPLITD SPLITB*. Because of that, with "DB" inventory control, four different ***G***(s) can be built. Each element of every ***G***(s) is found making a step change in an input variable while all other inputs are kept constant. It would not be correct to mix in the same ***G***(s) elements that correspond to one set of DOF with elements that correspond to another set of DOF.

For a DWC with "DB" inventory control, the four ***G***(s) have been calculated and the singular value decomposition has been applied to them in order to compare the controllability of the control structures. The separation of the mixture with α=(4.65 : 2.15 : 1) described in 4.11.1 (optimal operation) is chosen. The results for the L V S SPLITD PLITB set of DOF are shown in Table 4.13. According to singular value decomposition and ***RGA***, for the *L/D V S SPLITD SPLITB* set, *L/D V S* is found to be the preferred structure (*MRI*=0.06, *CN*=194). For *the L V/B S SPLITD SPLITB* set, *L V/B S* is found to be the preferred structure (*MRI*=0.11, *CN*=59). Finally, for the *L/D V/B S SPLITD SPLITB* set, *L/D V/B S* is found to be the preferred structure (*MRI*=0.06, *CN*=108). Comparing the four preferred structures, the best *II* is for the *L V S* structure (*MRI*=0.25, *CN*=91). Therefore, *L/D* and *V/B* variables do not appear in the set of preferred manipulated varialbes.

4.13 Conclusions

Considering diagonal feedback control, the DWC complex distillation arrangement offers some possibilities that have not been analysed in the literature and may have better controllability.

Despite the DWC non-linearity, linear DWC models expressed through the system transfer function are useful to study and compare different control structures within diagonal feedback control strategy. Several linear analysis tools such as the *MRI*, the *CN*, and the ***RGA*** among others are used to select appropriate control structures. A frequency analysis has permitted to give special importance to DWC response at the range of frequencies of interest. Non-linear

model simulations have been useful to test the controllers designed following linear considerations. Typical tuning methods are found to be limited for the tuning of the DWC.

The control of the logarithm of the product compositions instead of the control of the product compositions themselves may be a good alternative in the DWC. Improvement of the control performance has been proved for a specific example.

Controllability properties of the different stabilised DWC differ, what makes the consideration of different inventory control structures important. On the other hand, operating conditions have a large influence on the controllability of the system.

Comparing the separation of different mixtures in a DWC, it is found that the preferred control structures do not depend on the separated mixture. Therefore, some generality can be presumed. At optimal operating conditions, split variables (*SPLITD* and *SPLITB*) do not appear in the set of preferred manipulated variables. At non-optimal operating conditions, they do. In general, *MRI* and *CN* indicate that the controllability of structures with "LV" inventory control is better than the controllability of structures with "DB" inventory control. Specifically, the *CN* is very large for control structures with "DB" inventory controls, and small for control structures with "LV" inventory controls.

The "LV" stabilised DWC with *D S B* composition control structure meets good control properties. First of all, it has an inventory control which respects the rule of controlling the liquid levels in the tanks with *L* and V if the reflux ratios are large, as typically happens in the DWC. Secondly, it has good *MRI* and *CN*, and a well behaved ***RGA*** at the frequencies around the bandwidth. Finally, it presents large stability margins, what indicates robust stability.

Among the four proposed inventory control structures, the larger *MRI* and *CN* differences between optimal and non-optimal operating conditions are found for the "DB" stabilised DWC. According to the controllability indexes, the preferred control structures at optimal and non-optimal conditions are different. The controllability of the preferred control structure at non-optimal operating conditions is better. Therefore, it could be possible to renounce to energy savings in order to obtain better control performance. Split variables are included in the set of preferred manipulated variables at non-optimal operating conditions. The preferred control structure at optimal operating conditions is *L S V*. The inclusion of the split variables in the control structure permits to break the strong directionality of the *L S V* control structure, and makes the *CN* lower.